# DISTRIBUTED ALGORITHMS FOR SOURCE LOCALIZATION USING QUANTIZED SENSOR READINGS

by

Yoon Hak Kim

---

A Dissertation Presented to the
FACULTY OF THE GRADUATE SCHOOL
UNIVERSITY OF SOUTHERN CALIFORNIA
In Partial Fulfillment of the
Requirements for the Degree
DOCTOR OF PHILOSOPHY
(ELECTRICAL ENGINEERING)

December 2007

## Dedication

*To my mother for her support throughout my studies.*

*To my lovely wife, Hyun Bin for her constant love and encouragement.*

## Acknowledgments

First, I would like to thank my advisor, Prof. Antonio Ortega for his continual support, guidance and patience. It was the privilege to work with him during my doctoral research. Our discussions were crucial factors in accomplishing this work.

I would also like to thank Prof. Mitra and Prof. Govindan for being on my dissertation committee and Prof. Krishnamachari and Prof. Neely for serving on my qualifying examination committee. I am very grateful to them for their valuable comments and suggestions.

I would like to thank all my friends and colleagues for their help and friendship. My experience during the studies was much more enjoyable with them.

I would like to thank my mother who has devoted herself to my education since my childhood and my family, in particular my mother-in-law who always provided me with strong support throughout years. Finally, I would like to express my deepest gratitude to my wife Hyun Bin, for the unmeasurable love.

# Table of Contents

Dedication ii

Acknowledgments iii

List Of Tables vii

List Of Figures ix

Abstract xii

**Chapter 1: Introduction** 1
- 1.1 Motivation . . . 1
- 1.2 Related Work . . . 2
- 1.3 Distributed Algorithms for Source Localization System . . . 4
  - 1.3.1 Distributed Quantizer Design Algorithm . . . 5
    - 1.3.1.1 Rate Allocation . . . 6
  - 1.3.2 Distributed Localization Algorithm based on Quantized Data . . . 7
  - 1.3.3 Distributed Encoding Algorithm . . . 8
- 1.4 Outline and Contributions . . . 8

**Chapter 2: Quantizer Design** 11
- 2.1 Introduction . . . 11
- 2.2 Problem Formulation . . . 13
  - 2.2.1 Location Estimation based on Quantized Data . . . 15
  - 2.2.2 Criteria for Quantizer Optimization . . . 16
- 2.3 Quantizer Design Algorithm . . . 18
  - 2.3.1 Iterative Optimization Algorithm . . . 19
  - 2.3.2 Constrained Design Algorithm . . . 21
  - 2.3.3 Convergence and stopping criteria . . . 23
  - 2.3.4 Summary of algorithm . . . 24
- 2.4 Rate Allocation using GBFOS . . . 26
- 2.5 Application to Acoustic Amplitude Sensor Case . . . 28
  - 2.5.1 Source localization using quantized sensor readings . . . 28
  - 2.5.2 Quantizer design . . . 31
  - 2.5.3 Geometry-Driven Quantizers: Equally Distance-divided Quantizers 32

2.6 Simulation Results . . . 33
2.6.1 Quantizer design . . . 33
2.6.1.1 Comparison with traditional quantizers . . . 33
2.6.1.2 Comparison with optimized quantizers . . . 36
2.6.1.3 Sensitivity to parameter perturbation . . . 37
2.6.1.4 Performance analysis in a larger sensor network: comparison with traditional quantizers . . . 38
2.6.1.5 Discussion . . . 39
2.6.2 Rate allocation . . . 39
2.6.2.1 EDQ design . . . 39
2.6.2.2 Effect of quantization schemes . . . 41
2.6.2.3 Rate allocation under power constraints . . . 41
2.6.2.4 Performance analysis – comparison with uniform rate allocation . . . 42
2.6.2.5 Discussion . . . 45
2.7 Conclusion . . . 46

**Chapter 3: Localization Algorithm based on Quantized data** 47
3.1 Introduction . . . 47
3.2 Problem Formulation . . . 49
3.3 Localization Algorithm based on Maximum A Posteriori (MAP) Criterion: Known Signal Energy Case . . . 50
3.4 Implementation of Proposed Algorithm . . . 53
3.5 Unknown Signal Energy Case . . . 55
3.6 Simulation Results . . . 58
3.6.1 Case of known signal energy . . . 59
3.6.2 Case of unknown signal energy . . . 60
3.6.3 Sensitivity to parameter mismatches . . . 61
3.6.4 Performance analysis in a larger sensor network . . . 62
3.7 Conclusion . . . 63

**Chapter 4: Distributed Encoding Algorithm** 64
4.1 Introduction . . . 64
4.2 Definitions . . . 66
4.3 Motivation: Identifiability . . . 66
4.4 Quantization Schemes . . . 69
4.5 Proposed Encoding Algorithm . . . 70
4.5.1 Incremental Merging . . . 73
4.6 Extension of Identifiability: p-identifiability . . . 74
4.7 Decoding of Merged Bins and Handling Decoding Errors . . . 75
4.7.1 Decoding Rule 1: Simple Maximum Rule . . . 76
4.7.2 Decoding Rule 2: Weighted Decoding Rule . . . 77
4.8 Application to Acoustic Amplitude Sensor Case . . . 78
4.8.1 Construction of $S_Q(p)$ . . . 79
4.9 Experimental results . . . 80

4.9.1 Distributed Encoding Algorithm . . . . . 80
4.9.2 Encoding with p-Identifiability and Decoding rules . . . . . 83
4.9.3 Performance Comparison: Lower Bound . . . . . 86
4.10 Conclusion . . . . . 88

**Chapter 5: Conclusion and Future work** 90

Bibliography 93

## List Of Tables

Table 2.1 Comparison of LSQs with Optimized quantizers. The average localization error are computed using a test set of 2000 source locations. . . . 37

Table 2.2 Localization error (LE) of LSQ due to variations of the modelling parameters. LE $= \frac{1}{100}\sum_{l=1}^{100} E_l(\| \mathbf{x} - \hat{\mathbf{x}} \|^2)$, where $E_l$ is the average localization error for the $l$-th sensor configuration and is expressed in $m^2$. LE (normal) is for test set from normal distribution with mean of (5,5) and unit variance and LE (uniform) from uniform distribution. LSQs are designed with $R_i = 3, a = 50, \alpha = 2, g_i = 1$ and $w_i = 0$ for uniform distribution. . . . . 38

Table 2.3 Average localization error ($m^2$) vs. number of sensors ($M = 12, 16, 20$) in a larger sensor field, $20 \times 20m^2$. The localization error is averaged over 20 different sensor configurations where each quantizer uses $R_i = 3$ bits. . 39

Table 2.4 Localization error ($m^2$) for various sets of rate allocations where $\mathbf{R}^*_{EDQ}, \mathbf{R}^*_U$ and $\mathbf{R}^*$ are obtained by GBFOS using EDQ, uniform quantizer and LSQ, respectively given $\sum R_i = 10$. Localization error is computed by $E(\| \mathbf{x} - \hat{\mathbf{x}} \|^2)$ using EDQ and LSQ. . . . . 42

Table 2.5 Localization error ($m^2$) for various sets of rate allocations where $\mathbf{R}^*_{PW}$ was obtained by GBFOS using EDQ given $P = \sum_i C_i R_i = \sum_i 2C_i$. Localization error is given by $E(\| \mathbf{x} - \hat{\mathbf{x}} \|^2)$. . . . . 43

Table 3.1 Localization error (LE) ($m^2$) of MAP algorithm compared to energy ratios based algorithm (ERA) under various mismatches. In each experiment, a test set is generated with $M = 5$ and $\sigma = 0.05$ and one of the parameters is varied. Localization error (LE) ($m^2$) is computed by $E(\| \mathbf{x} - \hat{\mathbf{x}} \|^2)$ using $\alpha = 2, g_i = 1, R_i = 3$ and uniform distribution of $p(\mathbf{x})$. 62

Table 4.1 Total rate, $R_M$ in bits (Rate savings) achieved by various merging techniques. . . . . 82

Table 4.2 Total rate $R_M$ in bits (Rate savings) achieved by distributed encoding algorithm (global merging technique). The rate savings is averaged over 20 different node configurations where each node uses LSQ with $R_i = 3$. 83

# List Of Figures

Figure 1.1 Block diagram of source localization system. We assume the channel is noiseless and each sensor sends its quantized (Quantizer, $Q_i$) and encoded (ENC block) measurement to the fusion node where decoding and localization are conducted in a distributed manner. . . . . 2

Figure 2.1 Localization of the source based on quantized energy readings . . . 30

Figure 2.2 Comparison of LSQs with uniform quantizers and Lloyd quantizers. The average localization error is plotted vs. the number of bits, $R_i$, assigned to each sensor. The average localization error is given by $\frac{1}{500}\sum_{l}^{500} E_l(\|\mathbf{x}-\hat{\mathbf{x}}\|^2)$ where $E_l$ is the average localization error for the $l$-th sensor configuration. 2000 source locations are generated as a test set with uniform distribution of a source location. . . . . 34

Figure 2.3 Partitioning of sensor field ($10\times 10m^2$) (grid= $0.2\times 0.2$) by uniform quantizer (left) and Lloyd quantizer (right). 5 sensors are deployed with 2-bit quantizers. Each partition corresponds to the intersection region of 5 ring-shaped areas. More partitions yield better localization accuracy. . . 35

Figure 2.4 Partitioning of sensor field ($10 \times 10m^2$) (grid= $0.2 \times 0.2$) by EDQ (left) and LSQ (right). 5 sensors are deployed with 2-bit quantizers. Each partition corresponds to the intersection region of 5 ring-shaped areas. . . 35

Figure 2.5 Justification of EDQ design. The average localization error is plotted vs. the number of bits, $R_i$, assigned to each sensor with M=5 (left) and vs. the number of sensors, M with $R_i$ =3bits (right). The average localization error is given by $\frac{1}{500}\sum_{l}^{500} E_l(\|\mathbf{x}-\hat{\mathbf{x}}\|^2)$ where $E_l$ is the average of localization error for the $l$-th sensor configuration. 2000 source locations are generated as a test set with uniform distribution of source locations. . 40

Figure 2.6 Comparison of optimal rate allocation, $\mathbf{R}^*$ with uniform rate allocation $\mathbf{R}^U$. LSQs are designed for each $\mathbf{R}^*$ and $\mathbf{R}^U$. 4 curves are plotted for comparison. For example, "EDQ (or LSQ) with $\mathbf{R}^U$ (or $\mathbf{R}^*$)" indicates the curve of localization error computed when each sensor uses EDQ (or LSQ) designed for $\mathbf{R} = \mathbf{R}^U$ (or $\mathbf{R}^*$). . . . . 44

Figure 2.7 Gain in rate savings achieved by our optimal rate allocation, $\mathbf{R}^*$ using LSQs as compared with trivial solution where each sensor uses uniform quantizers of the same rate. . . . . 45

Figure 2.8 Evaluation of optimal rate allocation for many different sensor configurations. Localization error is averaged over 100 sensor configurations for two different rate allocations: $\mathbf{R}^U$ and $\mathbf{R}^*$. . . . . 46

Figure 3.1 Source locations that generate the given $\mathbf{Q_r}$ for each variance ($\sigma = 0, 0.05, 0.16, 0.5$) are plotted. 5 sensors (marked as $\circ$) are employed in a sensor field $10 \times 10m^2$ and each sensor uses a 2-bit quantizer. . . . . 53

Figure 3.2 Localization accuracy of proposed algorithm under source signal energy mismatch (top). In this experiment, a test set of 2000 source locations is generated for each source signal energy ($a = 40, 45, ..., 55, 60$). Localization is performed by the proposed algorithm in Section 3.4 using $a = 50$ and $\delta = 1m$. Distribution of weights vs. Number of weights chosen, $L$. (bottom) ($\frac{\sum_l^L W_l}{\sum_k^N W_k}$ vs. $L$). A test set of 2000 source locations is generated and N=10 weights are computed for each source location. . . . 59

Figure 3.3 Localization algorithms based on MMSE and MAP criterion are tested when $\sigma$ varies from 0.5 to 0 with $R_i = 3$ (left) and when $R_i = 3, 4$ and 5 with $\sigma = 0.05$ (right) and $\delta = 1m$ respectively. $w_i \sim N(0, \sigma^2)$. . . . 60

Figure 3.4 Localization algorithms based on MMSE estimation, MAP criterion and energy ratios are tested by varying source signal energy $a$ from 20 to 100. We set $N = 10, L = 3$, and $\delta_w = 1m$ in our algorithm. In this experiment, a test set with $M = 5, R_i = 3$ is generated with uniform distribution of source locations for each signal energy and the measurement noise is modeled by a normal distribution with zero mean and $\sigma = 0.05$. . 61

Figure 3.5 Localization algorithms based on MAP criterion and energy ratios are tested in a larger sensor network by varying the number of sensors. The parameters are $N = 10, L = 3$ and $\delta_w = 1m$ in our algorithm. In this experiment, a test set of 4000 samples was generated for $M = 12, 16, 20$. Each sensor uses a 3 bit quantizer and the measurement noise is modeled by the normal distribution with zero mean and $\sigma = 0.05$. . . . . 63

Figure 4.1 Encoder-Decoder Diagram . . . . . 75

Figure 4.2 Average localization error vs. Total rate $R_M$ for three different quantization schemes with distributed encoding algorithm. Average rate savings is achieved by the distributed encoding algorithm (global merging algorithm). . . . . 81

Figure 4.3 Average rate savings achieved by the distributed encoding algorithm (global merging algorithm) vs. number of bits, $R_i$ with $M = 5$ (left) and number of nodes with $R_i = 3$ (right) . . . . . 83

Figure 4.4 Rate savings achieved by the distributed encoding algorithm (global merging algorithm) vs. SNR (dB) with $R_i = 3$ and M=5. $\sigma^2 = 0, ..., 0.5^2$ . 84

Figure 4.5 Average localization error vs. total rate $R_M$ achieved by the distributed encoding algorithm (global merging algorithm) with simple maximum decoding and weighted decoding, respectively. Total rate varies by changing $p$ from 0.8 o 0.95 and weighted decoding is conducted with $L = 2$. Solid line + $\square$: weighted decoding. Solid line + $\nabla$: simple maximum decoding. . . . . 85

Figure 4.6 Average localization error vs. total rate, $R_M$ achieved by the distributed encoding algorithm (global merging algorithm) with $R_i = 3$ and M=5. $\sigma = 0, 0.05$. $S_Q(p)$ is varied from $p = 0.85, 0.9, 0.95$. Weighted decoding with $L = 2$ is applied in this experiment. . . . . 86

Figure 4.7 Performance comparison: distributed encoding algorithm is lower bounded by joint entropy coding. . . . . 88

## Abstract

We consider sensor-based distributed source localization applications, where sensors transmit quantized data to a fusion node, which then produces an estimate of the source location. For this application, the goal is to minimize the amount of information that the sensor nodes have to exchange in order to attain a certain source localization accuracy. We propose an iterative quantizer design algorithm that allows us to take into account the localization accuracy for quantizer design. We show that the quantizer design should be "application-specific" and a new metric should be defined to design such quantizers. In addition, we address, using the generalized BFOS algorithm, the problem of allocating rates to each sensor so as to minimize the error in estimating the position of a source.

We also propose a distributed encoding algorithm that is applied after quantization and achieves significant rate savings by merging quantization bins. The bin-merging technique exploits the fact that certain combinations of quantization bins at each node cannot occur because the corresponding spatial regions have an empty intersection.

We apply these algorithms to a system where an acoustic amplitude sensor model is employed at each sensor for source localization. For this case, we propose a distributed source localization algorithm based on the maximum a posteriori (MAP) criterion. If the source signal energy is known, each quantized sensor reading corresponds to a region in

which the source can be located. Aggregating the information obtained from multiple sensors corresponds to generating intersections between the regions. We develop algorithms that estimate the likelihood of each of the intersection regions. This likelihood can incorporate uncertainty about the source signal energy as well as measurement noise. We show that the computational complexity of the algorithm can be significantly reduced by taking into account the correlation of the received quantized data.

Our simulations show the improved performance of our quantizer over traditional quantizer designs and that our localization algorithm achieves good performance with reasonable complexity as compared to minimum mean square error (MMSE) estimation. They also show that an optimized rate allocation leads to significant rate savings (e.g., over 60%) with respect to a rate allocation that uses the same rate for each sensor, with no penalty in localization efficiency. In addition, they demonstrate rate savings (e.g., over 30%, 5 nodes, 4 bits per node) when our novel bin-merging algorithms are used.

# Chapter 1

# Introduction

## 1.1 Motivation

In sensor networks, multiple correlated observations are available from many sensors that can sense, compute and communicate. Often these sensors are battery-powered and operate under strict limitations on wireless communication bandwidth. This motivates the use of data compression in the context of various tasks such as detection, classification, localization and tracking, which require data exchange between sensors. The basic strategy for reducing the overall energy usage in the sensor network would then be to decrease the communication cost at the expense of additional computation in the sensors [42].

One important sensor collaboration task with broad applications is source localization. The goal is to estimate the location of a source within a sensor field where a set of distributed sensors measure the acoustic, seismic or thermal signals emitted by a source and manipulate the measurements to produce meaningful information such as signal energy, direction-of-arrival (DOA) and time difference-of-arrival (TDOA) [3, 20]. In such cases, the sensor observations are correlated and usually corrupted by noise. In addition,

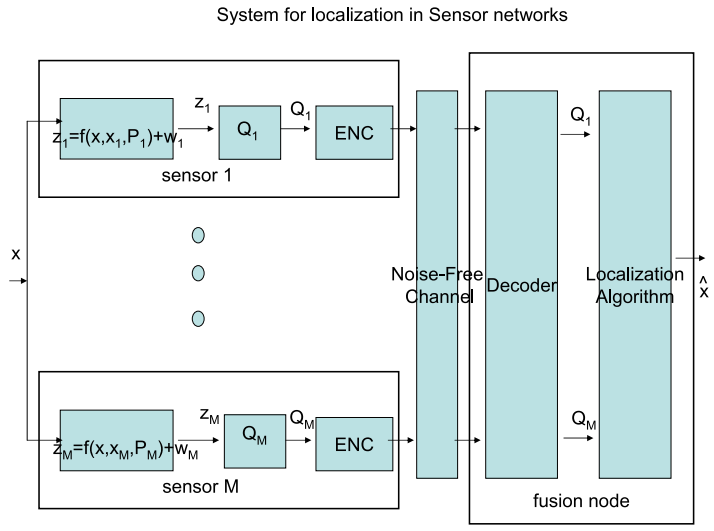


Figure 1.1: Block diagram of source localization system. We assume the channel is noiseless and each sensor sends its quantized (Quantizer, $Q_i$) and encoded (ENC block) measurement to the fusion node where decoding and localization are conducted in a distributed manner.

since there is normally a physical separation between the sensors and the fusion node, use of efficient data compression schemes becomes attractive for the sensor networks that normally have to operate under severely limited channel bandwidth.

It should be noted that since practical systems will require quantization of the observations before transmission, the estimation ought to be accomplished based on quantized observations. Thus, the goal of this thesis is to study the impact of quantization on the source localization performance of systems such as those in Figure 1.1.

## 1.2 Related Work

Localization algorithms based on acoustic signal energy measured at individual acoustic amplitude sensors have been proposed in [1, 11, 19, 30], where each sensor transmits un-

quantized acoustic energy readings to a fusion node, which then computes an estimate of the location of the source of these acoustic signals. Acoustic amplitude sensors are suitable for low cost systems such as sensor networks, even though measurements will be highly susceptible to environmental interference. The localization problem has been solved mostly through nonlinear least squares estimation, which is sensitive to local optima and saddle points. To overcome this drawback, alternative approaches that cast the problem as a convex feasibility problem have been proposed [1, 11].

Localization can also be performed using DOA sensors (sensor arrays) [2–4]. Sensor arrays generally provide better localization accuracy, especially in far-field, as compared to amplitude sensors, while they are computationally more expensive. TDOA can be estimated by using various correlation operations and a least squares (LS) formulation can be used to estimate source location [5, 24, 31]. Good localization accuracy for the TDOA method can be accomplished if there is accurate synchronization among sensors which may require communication overhead that could be significant in a wireless sensor network. It may be efficient to deploy different types of sensors (e.g., amplitude sensors and DOA sensors) in a sensor field of interest so that good localization accuracy can be achieved at reasonable cost [22].

None of these approaches take explicitly into account the effect of sensor reading quantization. Since the measurements should be quantized before transmission, estimation algorithms need to be developed based on quantized measurements. For example, in a simple distributed framework where a parameter of interest is directly estimated at each sensor, distributed estimators based on quantized data were derived in [23, 40]; these results rely on the availability of measurement noise statistics. In [25], the authors

considered a source localization system where each sensor measures the signal energy, quantizes it and sends the quantized sensor reading to a fusion node where the localization is performed. In this framework, the authors addressed the maximum likelihood (ML) estimation problem using quantized data and derived the Cramer-Rao bound (CRB) for comparison. Note that in deriving the ML estimator, it was assumed that each sensor used identical (uniform) quantizers. In [26], heuristic quantization schemes were also proposed in order to select the quantization to be used at all sensors. Note that this approach does not take into account the sensor location in order to assign quantizers to each sensor.

## 1.3 Distributed Algorithms for Source Localization System

We consider a situation where a set of sensors and a fusion node wish to cooperate to estimate a source location. We assume that each sensor can estimate noise-corrupted source characteristics, such as signal energy or DOA, using actual measurements (e.g., time-series measurements or spatial measurements). We also assume that there is only one way communication from sensors to fusion node, i.e., there is no feedback channel, the sensors do not communicate with each other (no relay between sensors) and these various communication links are reliable.

The block diagram for the source localization system we consider in this thesis is given in Figure 1.1. We propose distributed algorithms for quantizer design (the quantizers we design are $Q1, ..., Q_M$), encoding of quantized data (ENC) and localization (Localization Algorithm). We also address the problem of allocating the rate to each sensor so as to

minimize the localization error. We show that if the sensor location is known during the quantizer design process, significant performance gains can be achieved with respect to uniform quantization at all the sensors. In particular, it will be seen that optimal strategies for allocating bits to sensors tend to target a uniform "bit density" throughout the sensor field. Thus, the number of bits per sensor tends to be low in areas where many sensors are located, and conversely high where sensors are relatively far apart from each other.

### 1.3.1 Distributed Quantizer Design Algorithm

We address the quantizer design problem and propose an iterative algorithm for quantizer design ($Q_1, ..., Q_M$ in Figure 1.1). Since standard design of scalar quantizers aims at minimizing the average distortion between the actual sensor reading and its quantized value, there is no guarantee that these quantizers will reduce the localization error. Thus, we propose that quantizer design should be "application-specific". That is, to design such quantizers, a new metric should be defined that takes into account the accuracy of the application objective. Application specific quantizer designs have been proposed for several applications, including time-delay estimation [36, 37], speech recognition [33, 34], and speaker verification [35]. An overview of recent application specific quantization techniques can be found in [9]. In this thesis we consider as an application-specific metric the localization error, i.e., the difference between the actual source location and that estimated based on quantized data. A challenging aspect of this problem is that, while quantization has to be performed independently at each sensor, the localization error, which we wish to minimize, depends on the readings from *all* sensors. Thus we have a

problem where independent (scalar) quantizers for each sensor have to be designed based on a global (vector) cost function.

To solve this problem, we propose an iterative quantizer design algorithm for the localization problem (see [16, 18]), as an extension of our earlier work [32]. We apply our algorithm to a system where an acoustic sensor model proposed in [19] is considered. Our experiments demonstrate the benefits of using application-specific designs to replace traditional quantizers, such as uniform quantizers and Lloyd quantizers.

#### 1.3.1.1 Rate Allocation

Obviously, improved localization accuracy can always be achieved with finer quantization of the sensor measurements, but this requires higher overall power consumption for transmission, and thus potentially reduced lifetime for the sensors. Thus, we will explore the trade-off between rate (i.e., number of bits to represent the measurements) and overall localization accuracy. In [39], the authors considered an optimal power scheduling scheme which allowed them to determine the optimal rate for each sensor and thus the corresponding transmission power. In deriving the optimal scheme, they assumed that each sensor could measure directly the parameter to be estimated with error due to the measurement noise, and quantize its measurement using a uniform quantization scheme. However, in the case of source localization, each sensor can measure only the source signal (acoustic or seismic), from which estimates of signal energy or DOA can be obtained. Note that these measurements are nonlinear functions of the source location (the parameter to be estimated) and will be quantized before transmission to a fusion node. In addition, it will be generally more efficient to use different quantization schemes

at each sensor in order to achieve a certain degree of localization accuracy; this accuracy can vary significantly depending on the quantization scheme.

We address the rate allocation problem while taking into account the effect of quantization on localization. Clearly, better rate allocation can be achieved if better quantization schemes have been employed at each sensor. We apply the generalized BFOS algorithm (GBFOS [28]) to solve the problem. We perform the rate allocation for a system where an acoustic amplitude sensor model proposed in [19] is considered. Our rate allocation results indicate that better performance can be achieved when allocation leads to a partition of the sensor field that is as uniform as possible. Thus, when several sensors are clustered together, the rate per sensor tends to be lower than when the same sensors are more spread out.

### 1.3.2 Distributed Localization Algorithm based on Quantized Data

We address source localization problem based on quantized sensor readings when an acoustic amplitude sensor is employed at each sensor (see block Localization Algorithm in Figure 1.1). We show that when there is no measurement noise and known source signal energy, the localization is equivalent to computing the intersection of the regions, each of which corresponds to one quantized sensor reading from each sensor. In this thesis, we propose a distributed source localization algorithm that uses a maximum a posteriori (MAP) criterion (see [17]). To tackle this problem we use a probabilistic formulation, where we consider the likelihood that a given candidate source location would produce a given vector reading. We show that the complexity of the solution can be significantly reduced by taking into account the quantization effect and the distributed property of the

quantized data, without significant impact on localization accuracy. We also show that for the unknown source signal energy case, a good estimator of the source location can be found by computing a weighted average of the estimates obtained by our MAP-based algorithm under different source energy assumptions.

### 1.3.3 Distributed Encoding Algorithm

We propose a novel distributed encoding algorithm (blocks ENC and Decoder in Figure 1.1) that exploits redundancies in the quantized data from sensors and is shown to achieve significant rate savings, while preserving source localization performance [15]. With our method, we merge (non-adjacent) quantization bins in a given sensor whenever we determine that the ambiguity created by this merging can be resolved at the fusion node once information from other sensors is taken into account. Note that this is an example of binning as can be found in Slepian-Wolf and Wyner-Ziv techniques [7, 8, 12]. In our approach, however, we do not use any channel coding. Instead, we propose design techniques that allow us to achieve rate savings purely through binning, and provide several methods to select candidate bins for merging.

## 1.4 Outline and Contributions

The main contributions of this thesis are,

- Distributed Quantizer Design Agorithm

  We propose an iterative quantizer design algorithm which leads to quantizers that show improved performance over traditional quantizer designs. In addition, our

design algorithm can be combined with the rate allocation process to produce better results.

- Distributed Localization Algorithm

  We view the localization estimation problem as one of maximum a posteriori (MAP) detection problems so as to reduce the significant complexity that may be required by traditional estimators such as maximum likelihood (ML) and minimum mean square estimation (MMSE) estimators. We show that our distributed localization algorithm achieves good performance as compared with MMSE.

- Distributed Encoding Algorithm

  We propose a novel distributed encoding algorithm that merges quantization bins at each sensor and achieves rate savings without any loss of localization accuracy when there is no measurement noise. We show that a significant rate savings can be also obtained via our merging technique even when there is measurement noise.

The block diagram in Figure 1.1 illustrates the organization of the thesis. In Chapter 2 we address the problem formulation for designing quantizers (see block $Q_i, i = 1, ...M$ in Figure 1.1) and propose a distributed design algorithm that can be performed in an iterative fashion. We also show that significant gains can be obtained by using optimal rate allocation. In Chapter 3 we address the source localization problem based on quantized data and propose a distributed algorithm based on MAP criterion which shows good localization accuracy with reasonable complexity as compared with MMSE estimation (see block Localization Algorithm in Figure 1.1). In Chapter 4, assuming no measurement noise, we first present a novel encoding algorithm (block ENC in Figure 1.1) and further

develop decoding rules to resolve the decoding errors that may be caused by measurement noise or parameter mismatches. It should be noted that the decoding and the localization are conducted at the fusion node. As an example throughout this thesis, we consider a system where an acoustic amplitude sensor model is employed at each sensor. In each chapter, simulations are conducted to characterize the performance of our algorithms. Concluding remarks are given in Chapter 5.

# Chapter 2

# Quantizer Design

## 2.1 Introduction

In this chapter, we address a quantizer optimization problem where the goal is to design independent quantizers which operate on their sensor readings while they should minimize the localization error which depends upon all sensor readings. Instead of solving directly the problem by exhaustive search, we propose a distributed quantizer design algorithm which allows us to obtain independent quantizers by reducing the localization error in an iterative manner [6]. Similar procedures have been proposed for vector quantizer designs [21, 32]. We show that our iterative technique achieves performance close to the exhaustive search among independent quantizers.

We also address the rate allocation problem. We are given a total rate and each sensor is assigned additional rate iteratively until the total rate is fully allotted. To solve the problem we apply the generalized BFOS algorithm (GBFOS [28]) which requires calculation of Rate-Distortion (R-D) points for each candidate rate allocation. In addition, since power consumption due to rate transmission to the fusion node is proportional to

the distance between each sensor and the fusion node, the same rate at different sensors may lead to different power consumption. With this consideration, we also view the problem as a rate allocation under *power constraints* where the goal is to achieve optimal localization accuracy for a given power consumption. Note that the GBFOS algorithm allows us to choose the best rate allocation (R) that minimizes the localization error (D) computed using the quantized sensor readings, which are generated from any given set of quantizers designed for each candidate rate allocation. Thus, better rate allocation can be achieved if better quantizers have been employed at each sensor.

While the proposed quantizer design algorithm allows us to obtain good quantizers for each rate allocation, having to redesign the quantizers for each iteration of the rate allocation process would be computationally complex[1]. To avoid having to redesign quantizers at each iteration, we introduce "geometry-driven" quantizers, which are simple to implement and show good performance [16, 18].

In the experiments, we consider the acoustic amplitude sensor system (see [16–18]). Extensive simulations have been conducted to characterize the performance of our algorithm. Our experiments show the improved performance of our quantizers over traditional quantizers such as uniform quantizers and Lloyd quantizers. We also perform the rate allocation with several quantization schemes such as uniform quantizers, geometry-driven quantizers and the proposed quantizers. In the experiments, our rate allocation optimized

[1]Note that in some cases rate allocation and quantizer design can be done off-line, e.g., when the number and position of the sensors does not change, but that in many cases of interest the sensor network could be reconfigured regularly, e.g., some subsets of sensors would be activated, which would require on-line rate selection. In these latter cases, a low complexity rate allocation technique would be very important.

for source localization allowed us to achieve over 60% rate savings in some cases as compared to a uniform rate allocation, with no loss in localization accuracy.

This chapter is organized as follows. The problem formulation of the quantizer design is given in Section 2.2. An iterative quantizer design algorithm is proposed in Section 2.3 and the rate allocation using the GBFOS algorithm is described in Section 2.4. In Section 2.5, we present an application to the case where an acoustic amplitude sensor model is employed. Simulation results are given in Section 2.6 and the conclusions are found in Section 2.7.

## 2.2 Problem Formulation

Within the sensor field $S$ of interest, assume there are $M$ sensors located at known spatial locations, denoted $\mathbf{x}_i, i = 1, ..., M$, where $\mathbf{x}_i \in S \subset \mathbf{R}^2$. The sensors measure signals generated by a source located at an unknown location $\mathbf{x} \in S$, which we assume to be static during the localization process[2]. Denote $z_i$ the measurement at the $i$-th sensor over a time interval $k$:

$$z_i(\mathbf{x}, k) = f(\mathbf{x}, \mathbf{x}_i, \mathbf{P_i}) + w_i(k) \quad \forall i = 1, ..., M, \tag{2.1}$$

where $f(\mathbf{x}, \mathbf{x}_i, \mathbf{P_i})$ denotes the sensor model [3] employed at sensor $i$ and $w_i$ is a combined noise term that includes both measurement noise and modeling error. $\mathbf{P_i}$ is the parameter vector for the sensor model (an example of $\mathbf{P_i}$ for an acoustic amplitude sensor case is

[2]Obviously, our proposed techniques can be readily extended to the case where the source is moving and estimates of its location are computed independently at each time. Tracking algorithms that would exploit the spatial correlation of the source location go beyond the scope of this work.

[3]The sensor models for acoustic amplitude sensors and DOA sensors can be expressed in this form [22].

given in Section 2.5.1). It is assumed that each sensor measures its observation $z_i(\mathbf{x}, k)$ at time interval $k$, quantizes it and sends it to a fusion node, where all sensor readings are used to obtain an estimate $\hat{\mathbf{x}}$ of the source location.[4]

At sensor $i$ we use a $R_i$-bit quantizer with a dynamic range $[z_{i,min} \quad z_{i,max}]$. We assume that the quantization range can be selected for each sensor based on desirable properties of their respective sensing ranges. This will be illustrated in Section 2.5.2 with an example in the case of an acoustic amplitude sensor. Denote $\alpha_i(\cdot)$ the encoder at sensor $i$, which generates a quantization index $Q_i \in I_i = \{1, \ldots 2^{R_i}\}$. In what follows, $Q_i$ will also be used to denote the quantization bin to which measurement $z_i$ belongs. Denote $\beta_i(\cdot)$ the decoder corresponding to sensor $i$, which maps the quantization index $Q_i$ to a reconstructed quantized measurement $\hat{z}_i$.

Both this formulation and the subsequent design methodology are general and capture many scenarios of practical interest. For example, $z_i(\mathbf{x}, k)$ could be the energy captured by an acoustic amplitude sensor (this will be the case study presented in Section 2.5), but it could also be a DOA measurement.[5] Each scenario will obviously lead to a different sensor model $f(\mathbf{x}, \mathbf{x}_i, \mathbf{P_i})$. We assume that the fusion node needs observations, $z_i(\mathbf{x}, k)$, from *all* sensors in order to estimate the source location. In some cases one reading per sensor is used, while in other cases values of $z_i(\mathbf{x}, k)$ for several $k$'s are needed for localization. While multiple measurements can be made at each sensor, all individual measurements need not be sent. Instead, each sensor can compute a sufficient statistic

[4] In this thesis, we assume that $M$ sensors are activated prior to the localization process. However, selecting the best set of sensors for the localization accuracy would be important to improve the the system performance with limited energy budget [13, 38].

[5] In the DOA case each measurement at a given sensor location will be provided by an array of collocated sensors.

for localization from the multiple measurements, which can then be quantized and transmitted. For example, considering the case where the source is not moving and multiple source signal energy measurements are made, it can be easily shown that the average of the measurements at each sensor is a sufficient statistic for localization. Thus each sensor would simply quantize and transmit the average of its signal energy measurements. In what follows we discuss the design of a complete localization system, including i) source localization techniques that operate on quantized data, ii) quantizer design for localization, and iii) an algorithm to select the quantizer to use at each sensor.

### 2.2.1 Location Estimation based on Quantized Data

Clearly, for $z_i(\mathbf{x}, k)$ to be useful for localization it must be a function of the relative positions of the source and the sensor. Thus, there exists some function $g_u(\cdot)$ that can provide an estimate of the source location $\hat{\mathbf{x}}$ based on the original, unquantized, observations; these estimators have been the focus of most of the literature to date, for both sensor networks and other source localization scenarios. Instead, here our goal is to design both quantizers $\alpha_i$ *and* the corresponding estimators $g(\cdot)$ that operate on quantized data to estimate the source location $\hat{\mathbf{x}}$:

$$\hat{\mathbf{x}} = g(\alpha_1(z_1), ..., \alpha_M(z_M)). \tag{2.2}$$

While specific $g(\cdot)$ choices depend on the sensor model $f(\cdot)$, we can sketch some of their general properties (more details for a specific sensor model can be found in Section 2.5.1). First, $z_i(\mathbf{x}, k)$ must provide information (distance, angle, etc) about the relative position

of sensor and source. Thus, after quantization, each transmitted symbol will represent a *range* of positions (e.g., a range of distances from the sensor or an angular range). Second, with information obtained from all sensors, the source localization algorithm exploits the range information corresponding to each quantized symbol, $Q_i$. This is in general better than reconstructing $\hat{z}_i$ and then using reconstructed sensor information within a standard estimator, $g_u(\cdot)$. That is, an optimal estimator, $g(\cdot)$, should be a function of range information rather than reconstructed values.

In Section 2.5.1 we provide concrete examples for acoustic amplitude sensors in the noiseless case, and our more recent work [17] explores improved estimators that take into account the noise. In both cases, we derive optimal estimators in the minimum mean square error (MMSE) sense that make use of the range information, rather than the reconstructed values.

### 2.2.2 Criteria for Quantizer Optimization

We now consider, for a given rate allocated to each sensor, $\mathbf{R} = [R_1, ..., R_M]$, the problem of designing the scalar quantizers that can achieve maximum localization accuracy. Assume the sensor model, $f(\mathbf{x}, \mathbf{x}_i, \mathbf{P_i})$, and source localization function, $g(\cdot)$, are given. We define a cost function $J(\mathbf{x})$ for the quantizer design as follows:

$$J(\mathbf{x}) = \sum_{i}^{M} |z_i - \hat{z}_i|^2 + \lambda \parallel \mathbf{x} - \hat{\mathbf{x}} \parallel^2, \quad \forall \mathbf{x} \in S, \tag{2.3}$$

where $\hat{z}_i$ is the reconstructed value assigned to $z_i$ and $\hat{\mathbf{x}}$ is the estimated source location using a localization function $g(\cdot)$ that will also have to be designed. Note that the cost

function is a weighted sum of i) the standard mean squared error (MSE) in representing the sensor readings and ii) the localization error, $\| \mathbf{x} - \hat{\mathbf{x}} \|^2$. The Lagrange multiplier, $\lambda \geq 0$, controls the relative weight of these two cost metrics, so that when setting $\lambda = 0$, the problem of minimizing $J(\mathbf{x})$ becomes a standard quantizer design problem. Clearly, for the localization problem we address in this work, we could choose $\lambda = \infty$ since the goal is to design quantizers that minimize the localization error, $\|\mathbf{x} - \hat{\mathbf{x}}\|^2$ regardless of the MSE, $|z_i - \hat{z}_i^j|^2$.

However, in this chapter, we address the quantizer optimization problem using the weighted metric with a given $\lambda \neq 0$. This approach is chosen in order to limit the complexity of the quantizer design as will be described in what follows.

Recall that in our formulation we are designing *scalar* quantizers. Assume we are given a set of scalar quantizers, one for each sensor, and we seek to encode an observation in a way that minimizes the localization error. The key point to note is that the estimated location $\hat{\mathbf{x}}$ is based on *all* the quantized readings. Then, *localization optimized* encoding will in fact depend on the observations made at all the sensors. Thus it is likely that, in order to optimize localization, an observation $z_i$ at sensor $i$ will be assigned to different quantization bins depending on the observations at other sensors $z_j$ for $j \neq i$. Such an *unconstrained* encoder would achieve optimality in terms of localization but could only be used if there is information exchange between sensors, which has been precluded in our formulation because of the communication overhead it entails.

Instead we need to design a set of scalar quantizers that are *constrained*, in the sense that a given observation $z_i$ is always assigned to the same quantization index, no matter what the other sensor readings are. These are just standard scalar quantizers that apply

decision rules based on distance to encode $z_i$. Our goal is then to find the best scalar quantizer assignment by searching the set of all possible *constrained* quantizers.

Solving directly the problem (i.e., searching only among constrained quantizers) would require an exhaustive search and is not practical in general. Instead we will use iterative design techniques for a given $\lambda \neq 0$ in (2.3) where *we allow unconstrained quantizers to be used*. Within the design algorithm, mechanisms are then used to constraint the resulting quantizers. Essentially, this means that quantizers are designed so encoders minimize the metric of (2.3) with $\lambda \neq 0$, but are then approximated by encoders that operate based on $\lambda = 0$, as required for the real system (localization information is not known at the time of encoding).

While there will be a loss in localization performance relative to using unconstrained quantization, we will show examples to illustrate that our iterative techniques can achieve performance very close to exhaustive search among constrained quantizers.

## 2.3 Quantizer Design Algorithm

The goal of our quantizer design algorithm is to minimize the expected value of the cost function[6] in (2.3) where we average over all possible source locations, characterized by a probability density function $p(\mathbf{x})$:

$$J_{avg} = E(J(\mathbf{x})) = \int_S J(\mathbf{x})p(\mathbf{x})d\mathbf{x}. \tag{2.4}$$

[6]For source localization, the cost function $J(\mathbf{x})$ is replaced by the localization error $\| \mathbf{x} - \hat{\mathbf{x}} \|^2$.

If no prior information is available about the relative likelihood of possible source locations, $p(\mathbf{x})$ can be made uniform over the sensor field. For the purpose of training our quantizer, we generate a training set of observations $\{z_1(\mathbf{x},k),...,z_M(\mathbf{x},k)\}$ based on the sensor model, $f(\mathbf{x},\mathbf{x}_i,\mathbf{P_i})$, with a given choice of $p(\mathbf{x})$. Quantizer design is optimized for the known sensor locations and the given bit allocation. The optimal bit allocation will be discussed in Section 2.4.

In what follows we first explain the iterative optimization algorithm for the weighted metric with a given $\lambda$, then propose an iterative algorithm that allows us to consider unconstrained quantizers for quantizer design and finally we discuss convergence and stopping criteria for our algorithm.

### 2.3.1 Iterative Optimization Algorithm

The cost function $J(\mathbf{x})$ can then be rewritten in terms of the M quantizers and localization function $g(\cdot)$

$$J(\mathbf{x}) = \sum_{i}^{M} |z_i - \beta_i(\alpha_i(z_i))|^2 + \lambda \parallel \mathbf{x} - g(\alpha_1(z_1(\mathbf{x},k)),...,\alpha_M(z_M(\mathbf{x},k))) \parallel^2 . \tag{2.5}$$

We propose an iterative solution to search for $\alpha_i(\cdot), \beta_i(\cdot), g(\cdot), i = 1,...,M$ that minimizes $J_{avg}$ given by (2.4). For each sensor $i$ we optimize the quantizer selection, while quantizers for the other sensors remain unchanged. This is done successively for each sensor and repeated over all sensors until a stopping criterion is satisfied. Similar iterative procedures have been proposed for constrained product VQ design [32] and for entropy constrained

mean gain shape VQ [21]. Furthermore, in designing quantizers at each sensor, with the other quantizers fixed, we take the approach in [6]. That is, at sensor $i$ with $\beta_i(\cdot)$ and $g(\cdot)$ fixed, $\alpha_i(\cdot)$ is designed to minimize $J_{avg}(\alpha_i(\cdot), \beta_i(\cdot), g(\cdot), i = 1, ..., M) = J_{avg}(\alpha_i(\cdot))$. Similarly, $\beta_i(\cdot)$ (or $g(\cdot)$) is designed with $\alpha_i(\cdot)$ and $g(\cdot)$ (or $\alpha_i(\cdot)$ and $\beta_i(\cdot)$) fixed. If optimal solutions for each of these steps can be found, then this method guarantees that $J_{avg}(\alpha_i(\cdot), \beta_i(\cdot), g(\cdot))$ is nonincreasing at each step, thus leading to at least a locally optimal solution. We now describe solutions for each of these problems.

First, fix $\beta_i(\cdot)$ and $g(\cdot)$. The optimal encoder $\alpha_i^*(\cdot)$ that minimizes (2.5) (or equivalently, (2.4)) is such that:

$$\alpha_i^*(\cdot) = \arg\min_{\alpha_i(\cdot)} \int_{\mathbf{x}\in S} [|z_i - \beta_i(\alpha_i(\mathbf{x}))|^2 + \lambda \parallel \mathbf{x} - g(\alpha_i(\mathbf{x})) \parallel^2] p(\mathbf{x}) d\mathbf{x}. \tag{2.6}$$

Note that only the $i$-th MSE, $|z_i - \hat{z}_i|^2$ and the localization error $\|\mathbf{x} - \hat{\mathbf{x}}\|^2$ are affected by the selection of $\alpha_i^*(\cdot)$, i.e., all the other MSE terms are unchanged. Clearly, exhaustive search over all $\alpha_i(\cdot)$'s (with $\beta_i(\cdot)$ and $g(\cdot)$ fixed), guarantees that the overall cost would be non-increasing. This will be impractical, especially for high rates, but we will use such an exhaustive search in Section 2.6.1.2 to serve as a benchmark to evaluate the simpler techniques we propose in Section 2.3.2.

With $\alpha_i(\cdot)$ and $g(\cdot)$ fixed, the decoder $\beta_i^*(\cdot)$ that minimizes (2.5) is simply the centroid of all $z_i$ assigned to a specific quantization bin $Q_i^j$ for the $i$-th sensor[7], i.e.,

$$\beta_i^*(Q_i^j) = E[z_i(\mathbf{x}) | \mathbf{x} \in \{\mathbf{x} | \alpha_i(\mathbf{x}) = Q_i^j\}], \quad j = 1, ..., L_i, \forall_i \tag{2.7}$$

[7] note that $\beta_i^*(\cdot)$ only affects the MSE cost, since the localization estimate, $\hat{\mathbf{x}}$, is based on the quantization intervals.

Finally, given $\alpha_i(\cdot)$ and $\beta_i(\cdot)$, we can determine $g^*(\cdot)$ that minimizes (2.5) as follows:

$$g^*(\cdot) = \arg\min_{g(\cdot)} \int_{\mathbf{x}\in S} \| \mathbf{x} - g(\alpha_i(\mathbf{x})) \|^2 \, p(\mathbf{x}) d\mathbf{x} = \arg\min_{g(\cdot)} E[\| \mathbf{x} - \hat{\mathbf{x}} \|^2] \qquad (2.8)$$

Notice that the average localization error can be minimized by $g^*(\cdot) = E[\mathbf{x}|\alpha_1(\mathbf{x}), ..., \alpha_M(\mathbf{x})]$ which is the minimum mean square error (MMSE) estimator obtained given M encoders.

In summary, in our proposed iterative procedure two of the design steps can be solved optimally, while the remaining one (designing $\alpha_i(\cdot)$) can also be solved optimally, but would require an exhaustive search. It can be easily shown that for a given sensor each step in the optimization reduces overall cost and so the algorithm will converge to a minimum for the metric of (2.4). Moreover, when quantization for a sensor is optimized, the MSE of the other sensors is not affected, so that again overall cost is reduced. Thus a locally optimal solution can be found using this procedure. We next explain how an efficient constrained design for $\alpha_i$ can be obtained without requiring exhaustive search.

### 2.3.2 Constrained Design Algorithm

Suppose that at sensor $i$, we are given an encoder $\alpha_i = \{Q_i^j; j = 1, ..., L_i\}$ with $L_i = 2^{R_i}$ quantization levels. A partition $V_i = \{V_i^j; j = 1, ..., L_i\}$ analogous to the Voronoi partition in the generalized Lloyd algorithm is constructed as follows:[8]

$$V_i^j = \{\mathbf{x} : J(\mathbf{x}, \alpha_i = Q_i^j) \leq J(\mathbf{x}, \alpha_i = Q_i^m), \forall m \neq j\} \quad j = 1, ..., L_i \qquad (2.9)$$

[8] In the standard quantization ($\lambda = 0$), the Voronoi partition $V_i$ is equivalent to the encoder $\alpha_i$. That is, $V_i^j$ is the same region as the $j$-th quantization bin $Q_i^j$ and given by $V_i^j = \{z_i| \quad |z_i - \hat{z}_i^j|^2 \leq |z_i - \hat{z}_i^m|^2, \quad \forall m \neq j\}$.

where the cost function is computed using $\beta_i^*$ and $g^*(\cdot)$ which are obtained from (2.7) and (2.8) respectively. Notice that $V_i^j$ is a set of source locations that minimizes the cost function as mapped to $Q_i^j$. Then the average cost function $J_{avg}$ given in (2.4) can be computed using $V_i$ as follows:

$$J_{avg}(\alpha_i, V_i) = \sum_{j=1}^{L_i} E(J(\mathbf{x}, \alpha_i)|\mathbf{x} \in V_i^j) p(\mathbf{x} \in V_i^j) \tag{2.10}$$

$J_{avg}$ can be reduced by minimizing it for each $V_i^j$. As in the standard quantization ($\lambda = 0$), we perform the minimization over $\hat{z}_i^j$ for each $V_i^j$ which will be achieved by taking the centroid, $E(z_i(\mathbf{x})|\mathbf{x} \in V_i^j)$. Formally,

$$\begin{aligned} J_{avg}(\alpha_i, V_i) &\geq \sum_{j=1}^{L_i} \min_{\hat{z}_i^j} E(|z_i(\mathbf{x}) - \hat{z}_i^j|^2 + \lambda \|\mathbf{x} - g^*(\alpha_i)\|^2 | \mathbf{x} \in V_i^j) p(\mathbf{x} \in V_i^j) \\ &= J_{avg}(\alpha_i, \beta_i^*(V_i), V_i) \end{aligned} \tag{2.11}$$

where $\beta_i^*(V_i)$ produces the reconstructed values, $\hat{z}_i^j, j = 1, ..., L_i$ by taking the centroid over $\{z_i(\mathbf{x})|\mathbf{x} \in V_i^j\}$. It is noted that the encoding of sensor readings corresponding to $V_i$ in (2.9) is unconstrained since it requires knowledge of other sensor readings for encoding. Thus, the unconstrained encoder should be changed into the corresponding constrained one which in turn will be used for construction of $V_i$ at the next iteration. In our algorithm, we adopt a simple distance measure to obtain constrained encoders. We first find the centroid of each $V_i^j$ obtained from (2.9) and then use these centroids to create a quantization partition, i.e., a quantization bin $Q_i^j$ includes all inputs assigned to the centroid of $V_i^j$ using the nearest neighbor rule:

$$Q_i^j = \{z_i| \quad |z_i - \hat{z}_i^j|^2 \leq |z_i - \hat{z}_i^m|^2, \quad \forall m \neq j\} \tag{2.12}$$

where $\{\hat{z}_i^j | j = 1, ..., L_i\}$ generated from $\beta_i^*(V_i)$.

It should be noticed that the encoder $\hat{\alpha}_i = \{Q_i^j; j = 1, ..., L_i\}$ updated by (2.12) would not guarantee that the metric $J_{avg}$ is nonincreasing since the encoder $\hat{\alpha}_i$ is updated in a sense that only the first term $|z_i - \hat{z}_i^j|^2$ is minimized. That is, $\hat{\alpha}_i$ may increase the second term $\|\mathbf{x} - \hat{\mathbf{x}}\|^2 = \|\mathbf{x} - g^*(\hat{\alpha}_i)\|^2$ in $J_{avg}$. The procedure of (2.9) to (2.12) will be repeated at each sensor until a certain stopping criterion is satisfied.

### 2.3.3 Convergence and stopping criteria

The challenge for achieving convergence is that we need the unconstrained quantizers to minimize the metric with nonzero values of $\lambda$ while they should be replaced by the constrained ones which are not guaranteed to minimize the metric.[9] As in the standard quantization ($\lambda = 0$), we can seek to find the largest value $\lambda_{max}$ for $\lambda$ that leads directly to constrained encoding of sensor readings in order to guarantee convergence.

However, we observe that $\lambda_{max}$ tends to be very small and leads to localization errors that are greater than those achieved by first designing unconstrained quantizers and then forcing them to be constrained. This is not surprising since we design quantizers with small $\lambda$ while the localization error is minimized when $\lambda = \infty$.[10]

[9] We can do exhaustive search at each iteration to obtain the constrained quantizers that minimize the metric in order to guarantee the convergence but it would be too computationally expensive in practice.

[10] For some applications where the local metric (e.g., $|z_i - \hat{z}_i^j|^2$) and the global metric (e.g., $\|\mathbf{x} - \hat{\mathbf{x}}\|^2$) are important, we should be able to find $\lambda$ to maximize the application objective. For such cases, some techniques need to be developed to search for a reasonable $\lambda$.

In order to avoid increase in the metric at each iteration by (2.12), we suggest to use a simple stopping criterion which forces the algorithm to stop whenever the metric gets worse. This simple stopping rule would be efficient for the design of distributed quantizers for source localization since other quantizers are also designed so as to reduce the same metric, $\|\mathbf{x} - \hat{\mathbf{x}}\|^2$ and when the design process goes back again to say, $i$-th quantizer, the metric recomputed at sensor $i$ tends to get better than the previous iteration, making the algorithm continue to work. At least with this stopping criterion, we can guarantee that the metric is nonincreasing.

Despite the fact that $J_{avg}$ is not always nonincreasing due to (2.12), we can expect that the updated encoder $\hat{\alpha}_i$ will reduce the metric for most of iterations since it is updated based on the partition $V_i$ which is constructed in a sense that the metric is minimized.

As an example, we experiment with our quantizers for the acoustic amplitude sensor case in Section 2.6.1.1 where the algorithm is shown to produce a good solution on the average as compared with typical quantizers such as uniform quantizer and Lloyd quantizers. Our quantizers are also shown to achieve performance close to that of the optimized quantizers designed using the exhaustive search explained in Section 2.6.1.2.

### 2.3.4 Summary of algorithm

Given the number of quantization levels, $L_i = 2^{R_i}$, at sensor $i$, the algorithm is summarized as follows.[11]

**Algorithm 1** *For simplicity, in what follows, $z_i(\mathbf{x}, k)$ is written as $z_i(\mathbf{x})$.*

***Step1*** *: Initialize the encoders $\alpha_i(\cdot), i = 1, ..., M$. Set thresholds $\epsilon_1$ and $\epsilon_2$, set $i = 1$, and*

[11] Our algorithm can be applied for arbitrary integer, $L_i$, and not only those values corresponding to integer $R_i$.

*set iteration indices* $\kappa_1 = 1$ *and* $\kappa_2 = 1$.

***Step2*** *: Compute the cost function of (2.5).*

***Step3*** *: Construct the partition,* $V_i$ *using (2.9).*

***Step4*** *: Compute the average cost* $J_{avg}^{\kappa_1} = E[J(\mathbf{x})]$

***Step5*** *: If* $\frac{(J_{avg}^{\kappa_1 - 1} - J_{avg}^{\kappa_1})}{J_{avg}^{\kappa_1}} < \epsilon_1$ *go to Step 7; otherwise continue*

***Step6*** *:* $\kappa_1 = \kappa_1 + 1$. *Update the encoder* $\alpha_i$ *using (2.12). Go to Step 2*

***Step7*** *: if* $i < M \quad i = i + 1$ *go to step 2;*

*else if* $\frac{D^{\kappa_2 - 1}(\mathbf{x}, \hat{\mathbf{x}}) - D^{\kappa_2}(\mathbf{x}, \hat{\mathbf{x}})}{D^{\kappa_2}(\mathbf{x}, \hat{\mathbf{x}})} < \epsilon_2$ *Stop;*

*else* $i = 1; \kappa_2 = \kappa_2 + 1;$ *Go to Step 2,*

*where* $D^{\kappa_2}(\mathbf{x}, \hat{\mathbf{x}})$ *is given by* $E(\| \mathbf{x} - \hat{\mathbf{x}} \|^2)$ *at the* $\kappa_2$*-th iteration.*

Note that the quantizer design is performed off-line using a training set that is generated based on known values of $\mathbf{P_i}$ and $p(\mathbf{x})$; thus the quantizer training phase makes use of information about all sensors, but when the resulting quantizers are actually used, each sensor quantizes the information available to it *independently.*

It is possible to introduce "geometry-driven" quantizers: for the amplitude sensor case, these quantizers are designed so as to partition uniformly the distance between sensors and source (see Section 2.5.3). Similar ideas can be applied to DOA sensors, where quantizers provide uniform quantization of the angle of arrival. In Section 2.6, these quantizers are shown to be simple and achieve good performance as compared with the proposed quantizers. A discussion of the robustness of our quantizer to model mismatches is also left for Section 2.6.

## 2.4 Rate Allocation using GBFOS

With the proposed cost function we can design quantizers for a given rate allocation (bits assigned to each sensor). The next step is then to search for the rate allocation, $\mathbf{R}^*$, that minimizes the average localization error, i.e., $D = \int_{\mathbf{x}\in S} \|\mathbf{x} - \hat{\mathbf{x}}\|^2 p(\mathbf{x}) d\mathbf{x}$ for a given total rate $R_T = \sum_i^M R_i$.

A more general problem formulation can take into consideration transmission costs, e.g., the power consumption in the network required to transmit bits to the fusion node. This power consumption will depend on the bits allocated to specific sensors and also on the distance between these sensors and the fusion node. Thus, we can address the rate allocation problem under *power constraints* as follows: we are given a total power, $P = \sum_i^M P_i, P_i = C_i R_i$ where $C_i$ is the power required for sensor $i$ to transmit one bit to the fusion node, $\mathbf{x}_f$; Thus $P_i$ provides an approximation to the power consumption at sensor $i$. Our goal is then to find the rate allocation $\mathbf{R}^*$ that minimizes the average localization error for a given total power. Clearly, $C_i$ is proportional to the physical distance between $\mathbf{x}_i$ and $\mathbf{x}_f$ and thus once the sensors are deployed in a sensor field, it can be determined prior to the rate allocation[12]. Notice that only the relative values of $C_i$'s will play a role in this rate allocation process.

To solve the rate allocation problem for source localization, we can apply the well-known generalized BFOS algorithm (GBFOS) [28] to obtain $\mathbf{R}^*$. The algorithm typically starts by assigning the given maximum rate, $R_T$ to each sensor and then reduces the number of bits optimally until the rate budget is met. Initially, $R_i = R_T, i = 1, ..., M$

[12] $C_i$ can be written as $C_i = \gamma_i \parallel \mathbf{x}_f - \mathbf{x}_i \parallel^{\alpha_s}$ where $\alpha_s$ is the exponent for path-loss and $\gamma_i$ reflects transmission method and other factors [39]; in this chapter $\gamma_i$ is assumed to be equal for all sensors and thus ignored for simplicity.

and at each iteration we reduce the rate allocated to one of the sensors by computing alternative rate-distortion (R-D) operating points for each candidate rate allocation and choosing the one that minimizes the slope of the R-D curve. Note that as the bit rate is reduced, the distortion (localization error) at each sensor will decrease at different rates (equivalently, slope) in the R-D curve. This procedure guarantees the optimal reduction in bit rate at each iteration. This is done repeatedly until $\sum_i^M R_i = R_T$ is satisfied. Formally, at the $\eta$-th iteration,

$$i^\eta = \arg \min_{1 \le i \le M} \frac{D_i(\eta) - D(\eta - 1)}{\Delta R_i^\eta} \tag{2.13}$$

where $D(\eta - 1)$ is the average localization error at the previous step, $D_i(\eta) = \int_{\mathbf{x} \in S} \|\mathbf{x} - \hat{\mathbf{x}}^i(\eta)\|^2 p(\mathbf{x}) d\mathbf{x}$, $\hat{\mathbf{x}}^i(\eta)$ is computed using $g(\cdot)$ and M quantizers are designed for $\mathbf{R}^i = (R_1^\eta = R_1^{\eta-1}, ..., R_i^\eta = R_i^{\eta-1} - \Delta R_i^\eta, ..., R_M^\eta = R_M^{\eta-1})$.

Note that for each candidate rate allocation, we may design quantizers using the algorithm in Section 2.3.4 to achieve good rate allocation performance[13] or we can use simple quantization schemes that do not require redesigning quantizers at each iteration. For example, we can use $M$ uniform quantizers (or the "geometry-driven" quantizers to be introduced later) for the purpose of obtaining the rate allocation. Then, once an optimal rate allocation is obtained, a better set of quantizers can be designed for that rate using the algorithm in Section 2.3.4. Our experiments in Section 2.6 illustrate the impact of using different quantization schemes on the rate allocation performance. That is, it

[13]The rate allocation problem would be one of the applications where we can obtain benefits from using our quantizer design algorithm.

can be said that a significant gain can be achieved by taking into account quantization scheme during the rate allocation process.

The GBFOS algorithm can be also applied to the rate allocation problem under *power constraints*. In this case, at each step, we decrease the power consumed by individual sensors by reducing the bit rate assigned to them until $\sum_i C_i R_i = P$ is satisfied. That is, the same process as in the previous rate allocation will be performed except that the computation of the slope is conducted in terms of the power consumption so that at the $\eta$-th iteration,

$$i^{\eta} = \arg \min_{1 \le i \le M} \frac{D_i(\eta) - D(\eta - 1)}{\Delta P_i^{\eta}} \tag{2.14}$$

where $\Delta P_i^{\eta} = C_i \Delta R_i^{\eta}$.

## 2.5 Application to Acoustic Amplitude Sensor Case

### 2.5.1 Source localization using quantized sensor readings

Assuming no measurement noise ($w_i = 0$ in (2.1)), we consider source localization based on quantized data. Note that the localization algorithm to be explained in this section is designed for the high SNR regime ($w_i \approx 0$) but will also provide the foundation for localization based on noisy quantized data (see [17], and Chapter 3). Since each quantized sensor reading corresponds to a region where a source is located, all quantized sensor readings lead to a partition of a sensor field obtained by intersecting the regions corresponding to each sensor reading. Formally,

$$A = \bigcap_{i=i}^{M} A_i, \quad A_i = \{\mathbf{x} | f(\mathbf{x}, \mathbf{x}_i, \mathbf{P}_i) \in Q_i, \quad \mathbf{x} \in S\} \tag{2.15}$$

where $A_i$ is the region corresponding to the quantized reading from sensor $i$. Once the intersection region $A$ is obtained, we can compute the estimate as $\hat{\mathbf{x}} = E(\mathbf{x}|\mathbf{x} \in A)$. Notice that the estimator is optimal in MMSE sense under the assumption of no measurement noise.

As an example, we consider source localization based on acoustic sensor readings as proposed in [19], where an energy decay model of sensor signal readings is used for localization based on unquantized sensor readings.[14] This model is based on the fact that the acoustic energy emitted omnidirectionally from a sound source will attenuate at a rate that is inversely proportional to the square of the distance [27]. When an acoustic sensor is employed at each sensor, the signal energy measured at sensor $i$ over a given time interval $k$, and denoted by $z_i$, can be expressed as follows:

$$z_i(\mathbf{x}, k) = g_i \frac{a}{\|\mathbf{x} - \mathbf{x}_i\|^\alpha} + w_i(k), \tag{2.16}$$

where the parameter vector $\mathbf{P_i}$ in (2.1) consists of the gain factor of the $i$-th sensor $g_i$, an energy decay factor $\alpha$, which is approximately equal to 2, and the source signal energy $a$. The measurement noise term $w_i(k)$ can be approximated using a normal distribution, $N(0, \sigma_i^2)$. In (2.16), it is assumed that the signal energy, $a$, is uniformly distributed over the range $[a_{min} \quad a_{max}]$.

Assuming that the signal energy, $a$, is known,[15] localization based on quantized sensor readings can be illustrated by Figure 2.1, where each ring-shaped area corresponds to one quantized observation at a sensor. By computing the intersection of all the ring areas (one

[14] The energy decay model was verified by the field experiment in [19] and was also used in [11, 17, 22].

[15] In practice, the signal energy is unknown and should be jointly estimated along with the source location as described in [17] and in Chapter 3.

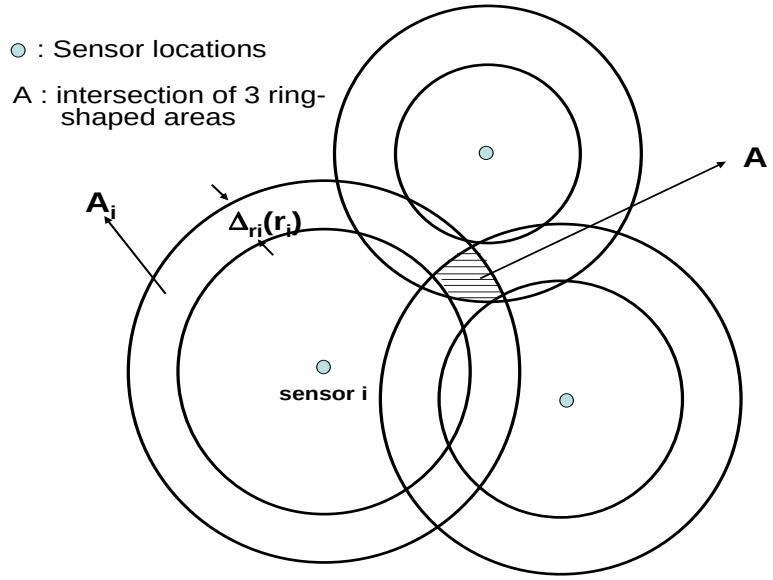


Figure 2.1: Localization of the source based on quantized energy readings

per sensor), it is possible to define the area where the source is expected to be located. Note that at least three observations are required to achieve a connected intersection and the region $A_i$ in (2.15) can be rewritten as follows:

$$\begin{aligned} A_i &= \{\mathbf{x} : g_i \frac{a}{\|\mathbf{x}-\mathbf{x}_i\|^\alpha} \in Q_i\} \\ \hat{\mathbf{x}} &= E(\mathbf{x}|\mathbf{x} \in \bigcap_i^M A_i), \end{aligned} \tag{2.17}$$

where $A_i$ is the ring-shaped region obtained from the quantized bin $Q_i$ that $z_i$ falls into (Figure 2.1). If the source is uniformly distributed in the sensor field, the estimate, $\hat{\mathbf{x}}$ would be the sample mean in the intersection $A$. Clearly, $\hat{\mathbf{x}}$ is the MMSE estimator under the assumption of known energy and no measurement noise.

A similar approach can be applied to the DOA sensor case where each quantized sensor reading leads to a cone-shaped region and the localization will be performed by computing the intersection of the corresponding regions.

### 2.5.2 Quantizer design

In quantizer design, we generate the training set assuming that the signal energy $a$ is known and $w_i = 0$. Notice that $M$ quantizers $(\alpha_1, ..., \alpha_M)$ are designed by reducing the metric, $J(\alpha_i, \beta_i^*, g^*(\cdot))$ with $\lambda = \infty$ at each iteration where $\beta_i^*$ and $g^*(\cdot)$ are given by (2.7) and (2.17), respectively. However, since the signal energy is generally unknown, the sensitivity to mismatches in signal energy will be studied in Chapter 3, where localization algorithms will be developed to handle measurement noise and unknown signal energy.

Since the signal energy takes any value in the range $[a_{min} \quad a_{max}]$ in real situations, quantizers should be designed to avoid quantizer overload by setting the dynamic ranges of the $M$ quantizers as $[z_{i,min} \quad z_{i,max}] = [\frac{a_{min}}{r_{i,max}^2} \quad \frac{a_{max}}{r_{i,min}^2}]$ where $[r_{i,min} \quad r_{i,max}]$ is the range within which the $i$-th sensor is supposed to measure acoustic source energy. The value of $r_{i,max}$ can be set such that the probability that an arbitrary point inside the sensor field is sensed simultaneously by at least 3 sensors should be close to 1 [41]. Assuming that the distribution of the number of sensors in any given circle with area $C_d = \pi r_d^2$ is Poisson with rate $\lambda_d C_d$ where $\lambda_d$ is the sensor density (sensors/$m^2$), the probability $p$ is then given by

$$p = \sum_{i=3}^{\infty} \frac{e^{-\lambda_d \pi r_d^2} (\lambda_d \pi r_d^2)^i}{i!} \tag{2.18}$$

Given $\lambda_d$, we can compute $r_{i,max} (\geq r_d)$ for a desirable value of $p$ (say, 0.999). In this way, the likelihood of missing a source is minimized. In order to guarantee that finite dynamic ranges are used, the value of $r_{i,min}$ is chosen as a small nonzero value ($0.2 \leq r_{i,min} \leq 1.0m$). Note that if more sensors are used, better quantization in each sensor is possible

(the dynamic ranges will tend to be smaller). With this initialization step, the quantizer design as outlined in Section 2.3.4 can be used.

### 2.5.3 Geometry-Driven Quantizers: Equally Distance-divided Quantizers

Since each set of quantizers induces a partitioning of the sensor field, designing good quantizers for localization can be seen to be equivalent to making a good partition of the sensor field by adjusting the width, $\Delta_{r_i}(r_i)$, of the ring-shaped areas in Figure 1. If no prior information is available about the source location, $p(x)$ can be assumed to be uniform and thus choosing $\Delta_{r_i}(r_i)$ to achieve a uniform partitioning of the sensor field would seem to be a good choice. Intuitively, a uniform partitioning of the sensor field is more likely to be achieved when the ring-shaped areas have the same width, $\Delta_{r_i}(r_i) = const$ (this is certainly the case when the sensors are uniformly distributed). This consideration leads us to introduce equally distance-divided quantizers (EDQ), which can be viewed as uniform quantizers in distance such that $\Delta_{r_i}(r_i) = \frac{r_{i,max} - r_{i,min}}{L_i}, \forall i$. That is, EDQ allows each sensor to quantize the signal intensity such that the rings have equal width. To justify the EDQ design, we performed a simulation (see Figure 2.5) that shows that EDQ provides good localization performance, which comes close to that achievable by the quantizers proposed in Section 2.3.4. EDQ has the added advantage of facilitating the solution of the rate allocation problem. While the GBFOS algorithm [28] provides the optimal rate allocation, it would also require very large computational load, since it relies on the calculation of rate-distortion points at each iteration step, and the quantizers should be redesigned using the algorithm of Section 2.3.4 for each candidate rate allocation. Instead, in our experiments we use the GBFOS algorithm along with

EDQ, which does not require quantizer redesign for each candidate rate allocation. With this approach one can use EDQ to compute easily the optimal rate allocation for the particular sensor configuration, and then use the technique proposed in Section 2.3.4 to design a quantizer for the given optimal rate allocation.

## 2.6 Simulation Results

In our experiments, we denote localization-specific quantizer (LSQ) the quantizer designed using the algorithm proposed in Section 2.3.4 and assume that each sensor uses the same dynamic range with $r_{i,min} = 1m$ and $r_{i,max} = r_d$ (see Section 2.5.2 for details of the dynamic range) for all quantizers (uniform quantizer, Lloyd quantizer, EDQ and LSQ).

### 2.6.1 Quantizer design

We design LSQs using a training set including 1500 source locations generated with a uniform distribution in a sensor field of size $10 \times 10m^2$, where $M = 3, 4, 5$ sensors are randomly located. In these experiments, the cost function is given by $J = \| \mathbf{x} - \hat{\mathbf{x}} \|^2$ (equivalently, $\lambda = \infty$ in (2.3)) and the model parameters are $a = 50, \alpha = 2, g_i = 1$ and $\sigma_i^2 = 0$. Note that Lloyd quantizers are designed with $\lambda = 0$ in (2.3). We evaluate the results in terms of the average localization error, $E(\| \mathbf{x} - \hat{\mathbf{x}} \|^2)$ computed by (2.17).

#### 2.6.1.1 Comparison with traditional quantizers

In Figure 2.2, LSQ is compared with traditional quantizers such as uniform quantizers and Lloyd quantizers in terms of the average localization error. In this experiment, 500 different sensor configurations are generated for $M = 3, 4, 5$, and for each configuration LSQs

are designed for $R_i = 2, 3, 4$. The 95% confidence interval for the localization error is also plotted to show the robustness of LSQ to the sensor configuration. It can be noted that LSQ is more robust than traditional quantizers, since the sensor configuration is already taken into account in the LSQ design. In contrast, the other quantizers are designed without considering sensor location information. Because of this, they may perform poorly in certain sensor configurations, thus leading to greater variance in localization error than with LSQ.

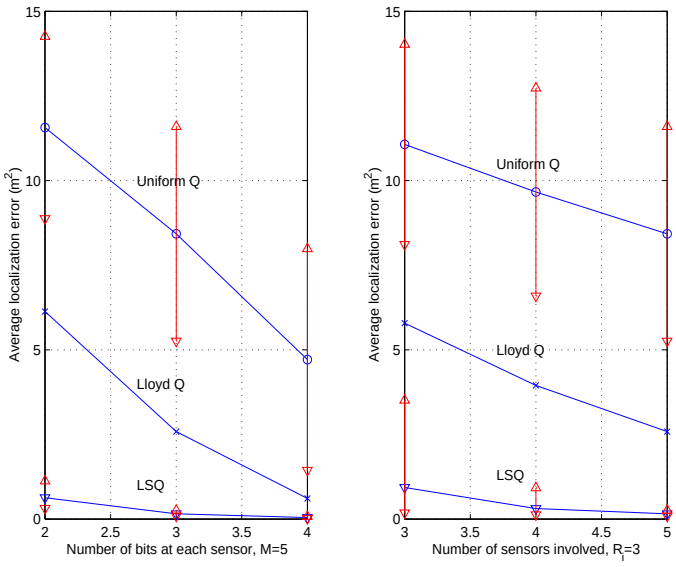


Figure 2.2: Comparison of LSQs with uniform quantizers and Lloyd quantizers. The average localization error is plotted vs. the number of bits, $R_i$, assigned to each sensor. The average localization error is given by $\frac{1}{500}\sum_{l}^{500} E_l(\|\mathbf{x} - \hat{\mathbf{x}}\|^2)$ where $E_l$ is the average localization error for the $l$-th sensor configuration. 2000 source locations are generated as a test set with uniform distribution of a source location.

Since LSQ makes full use of the distributed property of the observations, it can be seen to provide improved performance over traditional quantizers. This can be also explained in terms of the partitioning of the sensor field, as shown in Figures 2.3 and 2.4. As expected, the ring-shaped areas for uniform quantizers are hardly overlapped, yielding

the worst partitioning of a sensor field, since most quantization bins are mapped into regions close to the sensors by the relation, $z_i \propto \frac{1}{r_i^2} = \frac{1}{\|\mathbf{x}-\mathbf{x}_i\|^2}$. It is also easily seen that LSQ leads to a more uniform partitioning, which in turn reduces the localization error.

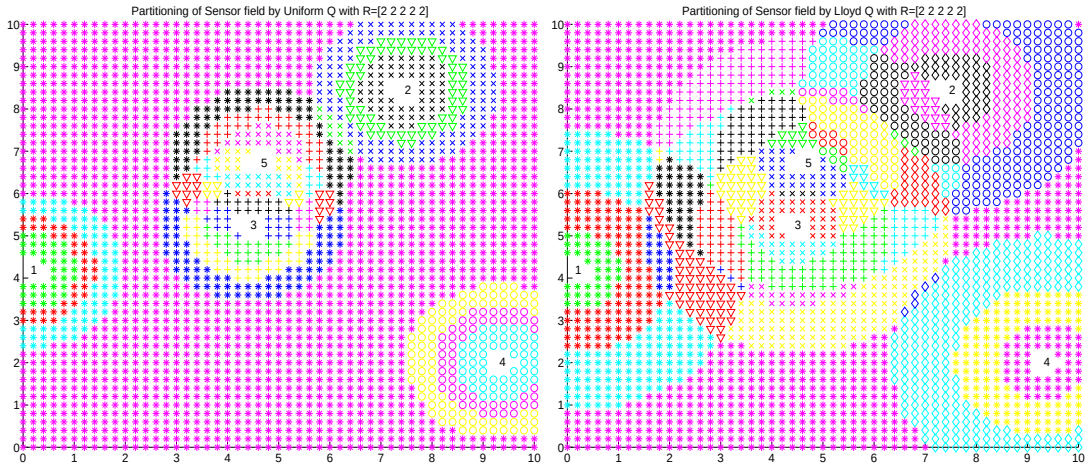


Figure 2.3: Partitioning of sensor field ($10 \times 10m^2$) (grid= $0.2 \times 0.2$) by uniform quantizer (left) and Lloyd quantizer (right). 5 sensors are deployed with 2-bit quantizers. Each partition corresponds to the intersection region of 5 ring-shaped areas. More partitions yield better localization accuracy.

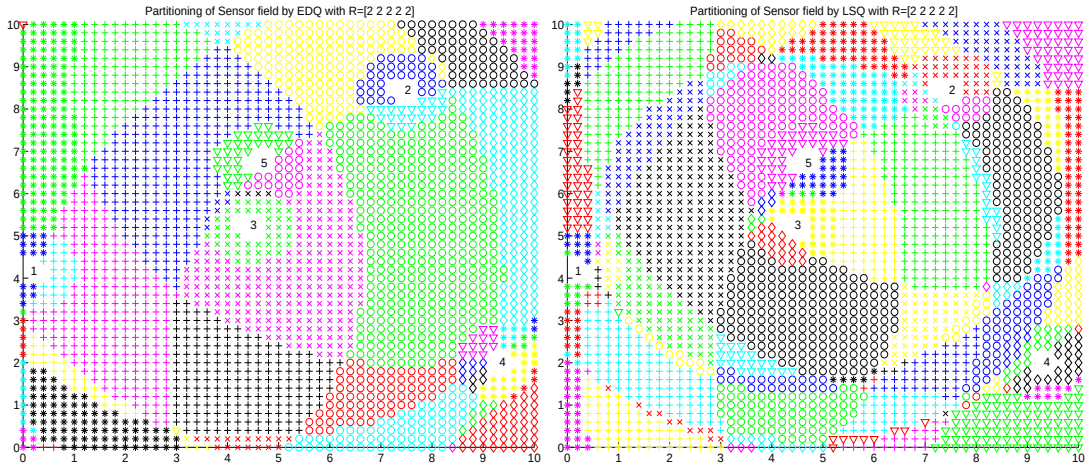


Figure 2.4: Partitioning of sensor field ($10 \times 10m^2$) (grid= $0.2 \times 0.2$) by EDQ (left) and LSQ (right). 5 sensors are deployed with 2-bit quantizers. Each partition corresponds to the intersection region of 5 ring-shaped areas.

#### 2.6.1.2 Comparison with optimized quantizers

LSQs are also compared to optimized quantizers which are designed by an exhaustive search. In this experiment, since the computational complexity required to search for $\alpha_i^*$ in (2.6) is very high, we make some approximations to curtail the search size. That is, each encoder, $\alpha_i^*$ is designed based on two different methods which approximate the exhaustive search.

- Method 1: first, we search over $\alpha_i$ which are constructed with a coarse grid $\Delta_c = \frac{z_{i,max}-z_{i,min}}{N_s}$ where $N_s$ determines the size of the set $\{\alpha_i\}$ computed by $\frac{N_s!}{(L_i-1)!(N_s-L_i+1)!}$. Once we obtain the encoder with $\Delta_c$, we observe that the boundary values that determine quantization bins are located in the subinterval, $[z_{i,min} \quad z_i^h], \quad z_i^h \ll z_{i,max}$. Thus, we search using a fine grid, $\Delta_f = \frac{|z_i^h - z_{i,min}|}{N_s}, \Delta_f \ll \Delta_c$ with reduced complexity to find the encoder that minimizes the metric given by (2.6).

- Method 2: instead of searching with a fixed grid size, we consider a variable grid size that allows us to search with finer grid over the encoders that show good performance. That is, by using the grid $\Delta_r = \frac{r_{i,max}-r_{i,min}}{N_r}$, we can construct candidate encoders with their quantization bins that uniformly divide the sensor field (for further details, see EDQ in Section 2.5.3). It is noted that the search grid mapped from $\Delta_r$ becomes smaller toward $z_{i,min}$ and larger toward $z_{i,max}$.

For the same sensor configuration of Figure 2.4, the optimized quantizers are designed with $R_i = 2$ and tested for comparison. The number of partitions and the localization error are tabulated for several quantizers in Table 2.1. OPT Q1 and OPT Q2 correspond to the quantizers designed using Method 1 and Method 2, respectively. For comparison, the

search grids for the optimized quantizers are determined such that the search complexity for them is almost the same. Note that more partitions tend to yield better localization accuracy. It can be seen that LSQ achieves performance close to the optimized ones, both in terms of average localization error and in number of partitions.

Table 2.1: Comparison of LSQs with Optimized quantizers. The average localization error are computed using a test set of 2000 source locations.

| Quantizer Type | Uniform Q | Lloyd Q | LSQ | OPT Q1 | OPT Q2 |
|---|---|---|---|---|---|
| Number of partitions | 36 | 55 | 132 | 140 | 142 |
| Avg. Localization error | 11.1172 | 6.0463 | 0.3758 | 0.3088 | 0.3001 |

#### 2.6.1.3 Sensitivity to parameter perturbation

LSQ was evaluated under various types of mismatch conditions for 100 different 5-sensor configurations. In each test we modified one of the parameters with respect to what was assumed during quantizer training. The simulation results are tabulated in Table 2.2. In this experiment, 1000 source locations in a sensor field $10 \times 10m^2$ were generated under assumptions of both a uniform distribution and a normal distribution for each configuration. We assume that the true parameters can be estimated at the fusion node and used for localization. Note that our localization algorithms are not very sensitive to parameter mismatches (see [17] and Chapter 3). Thus, small errors in estimating parameters at the fusion node from received quantized data do not lead to significant localization errors.

As seen in Table 2.2, LSQ is robust to mismatch situations where the parameters used in quantizer design are different from those characterizing the simulation conditions.

Thus, there would be no need to redesign the quantizers when the parameter mismatches are small.

Table 2.2: Localization error (LE) of LSQ due to variations of the modelling parameters. LE $= \frac{1}{100}\sum_{l=1}^{100} E_l(\| \mathbf{x}-\hat{\mathbf{x}} \|^2)$, where $E_l$ is the average localization error for the $l$-th sensor configuration and is expressed in $m^2$. LE (normal) is for test set from normal distribution with mean of (5,5) and unit variance and LE (uniform) from uniform distribution. LSQs are designed with $R_i = 3, a = 50, \alpha = 2, g_i = 1$ and $w_i = 0$ for uniform distribution.

| Decay factor $\alpha$ | 1.8 | 1.9 | 2 | 2.1 | 2.2 |
|---|---|---|---|---|---|
| LE (normal) | 0.4654 | 0.2211 | 0.1468 | 0.3512 | 1.1254 |
| LE (uniform) | 1.7025 | 0.5586 | 0.1321 | 0.4612 | 1.4235 |
| Gain factor $g_i$ | 0.8 | 0.9 | 1 | 1.1 | 1.2 |
| LE (normal) | 0.5567 | 0.2332 | 0.1468 | 0.1521 | 0.2783 |
| LE (uniform) | 0.6734 | 0.2556 | 0.1321 | 0.2298 | 0.5176 |

#### 2.6.1.4 Performance analysis in a larger sensor network: comparison with traditional quantizers

Since there are a large number of sensors in a typical sensor network, we now evaluate LSQ for large sensor networks. In this experiment, 20 different sensor configurations in a larger sensor field, $20 \times 20m^2$, are generated for $M = 12, 16, 20$. For each sensor configuration, LSQs are designed with a given rate of $R_i = 3$ and show good performance with respect to traditional quantizers in Table 2.3. Note that the sensor density for $M = 20$ in $20 \times 20m^2$ is equal to $\frac{20}{20\times 20} = 0.05$ which is that for the case of $M = 5$ in $10 \times 10m^2$. It is worth noting that the system with a larger number of sensors outperforms the system with a smaller number of sensors ($M = 3, 4, 5$) although the sensor density is kept the same. This is because localization performance degrades around the edges of the sensor field

and thus in a larger sensor field there is a relatively smaller number of source locations near the edge, as compared to a smaller field with the same sensor density.

Table 2.3: Average localization error ($m^2$) vs. number of sensors ($M = 12, 16, 20$) in a larger sensor field, $20 \times 20m^2$. The localization error is averaged over 20 different sensor configurations where each quantizer uses $R_i = 3$ bits.

| Number of sensors, $M$ | Uniform Q | Lloyd Q | LSQ |
|---|---|---|---|
| 12 | 2.6007 | 0.7152 | 0.1105 |
| 16 | 1.7386 | 0.3976 | 0.0708 |
| 20 | 0.9541 | 0.2284 | 0.0525 |

#### 2.6.1.5 Discussion

Based on the above experiments, we make the following observations. First, each sensor should use a different quantizer, designed based on the location of all sensors to achieve good localization accuracy. Second, the proposed algorithm provides a practical way of designing independent quantizers that reduce a global metric (localization error) without requiring exhaustive search.

### 2.6.2 Rate allocation

#### 2.6.2.1 EDQ design

Before employing the EDQs for the rate allocation problem, we compare their performance to that of LSQs. Refer to Figure 2.5, where 500 different sensor configurations are generated for each $M$ ($M = 3, 4, 5$) and LSQ and EDQ are compared with a test set of 2000 source locations for each configuration. Figure 2.5 shows that EDQ provides good localization performance, which comes close to that achievable by LSQ. In Figure 2.4,

the partitioning of a $10 \times 10m^2$ sensor field with 5 sensors deployed is plotted for EDQ and LSQ respectively.

Based on these experiments we observe that EDQ allows us to achieve a good partitioning, even though the sensor location information is not taken into account for EDQ design. Note that the benefit of LSQ design will become insignificant as rate and/or number of sensor increases. (see Figures 2.2 and 2.5). This is because each partition (equivalently, the intersection of M ring-shaped areas) becomes smaller when the number of sensors and/or the rate increases and thus there will be less gain to be achieved by making each partition as equal in area as possible during LSQ design

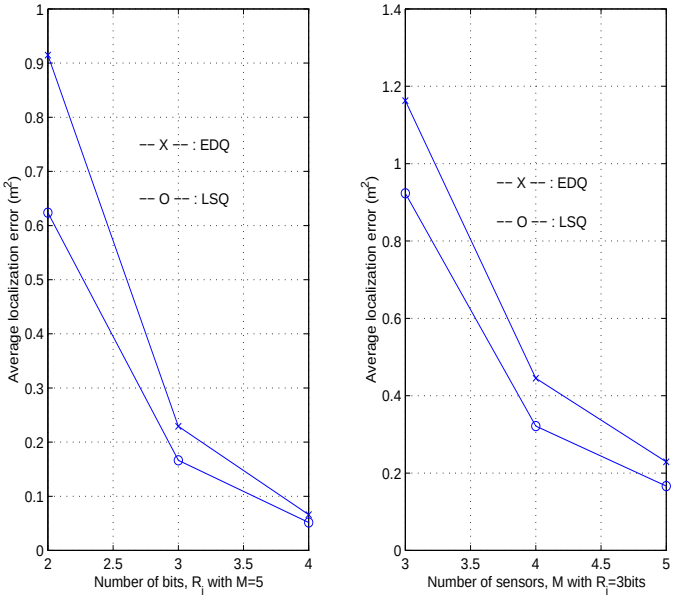


Figure 2.5: Justification of EDQ design. The average localization error is plotted vs. the number of bits, $R_i$, assigned to each sensor with M=5 (left) and vs. the number of sensors, M with $R_i$ =3bits (right). The average localization error is given by $\frac{1}{500}\sum_l^{500} E_l(\|\mathbf{x}-\hat{\mathbf{x}}\|^2)$ where $E_l$ is the average of localization error for the $l$-th sensor configuration. 2000 source locations are generated as a test set with uniform distribution of source locations.

#### 2.6.2.2 Effect of quantization schemes

In the same sensor configuration as in Figure 2.3, the rate allocation was conducted using three different quantizers (uniform quantizers, EDQs and LSQs) to search for the optimal rate allocation that would give the minimum localization error. In the example of Figure 2.3, it can be seen that sensors 3 and 5 are so close to each other that they provide redundant information for localization and thus the optimal solution allocates few bits to both these sensors. In fact, in our example, at relatively low rates (an average of 2 bits per sensor) it is more efficient to send information from only three sensors (sensors 1,2 and 4), i.e., allocating zero bits for the other two sensors (sensors 3 and 5). The results obtained by the rate allocation are provided in Table 2.4 where the localization errors were computed using EDQs and LSQs designed for several different rate allocations, demonstrating that rate allocation is important to achieve good localization performance. To test the effect of different quantization schemes at each sensor, the rate allocation was conducted using uniform quantizers, EDQs and LSQs at each sensor to obtain $\mathbf{R}_U^*, \mathbf{R}_{EDQ}^*$ and $\mathbf{R}^*$, respectively. Note that the same rate allocation ($\mathbf{R}^* = \mathbf{R}_{EDQ}^*$) was obtained for EDQs and LSQs.

#### 2.6.2.3 Rate allocation under power constraints

The rate allocation under power constraints given by (2.14) was also performed using EDQs for the sensor configuration in Figure 2.3. In this experiment, the fusion node $\mathbf{x}_f$, is assumed to be located at $(10, 10)$ and the power consumption at sensor $i$ is assumed to be $P_i = C_i R_i = \|\mathbf{x}_i - \mathbf{x}_f\|^{\alpha_s} R_i$ where $\alpha_s = 1$ for simplicity. The optimal rate allocation

Table 2.4: Localization error ($m^2$) for various sets of rate allocations where $\mathbf{R}^*_{EDQ}, \mathbf{R}^*_U$ and $\mathbf{R}^*$ are obtained by GBFOS using EDQ, uniform quantizer and LSQ, respectively given $\sum R_i = 10$. Localization error is computed by $E(\| \mathbf{x} - \hat{\mathbf{x}} \|^2)$ using EDQ and LSQ.

| Sets of rate allocations | EDQ | LSQ |
|---|---|---|
| $\mathbf{R}^* = [4 \quad 3 \quad 0 \quad 3 \quad 0]$ | 0.1533 | 0.1226 |
| $\mathbf{R}^*_{EDQ} = [4 \quad 3 \quad 0 \quad 3 \quad 0]$ | 0.1533 | 0.1226 |
| $\mathbf{R} = [3 \quad 3 \quad 0 \quad 4 \quad 0]$ | 0.1615 | 0.1258 |
| $\mathbf{R} = [3 \quad 4 \quad 0 \quad 3 \quad 0]$ | 0.1543 | 0.1329 |
| $\mathbf{R} = [3 \quad 2 \quad 2 \quad 3 \quad 0]$ | 0.3005 | 0.2297 |
| $\mathbf{R} = [2 \quad 2 \quad 2 \quad 2 \quad 2]$ | 0.6199 | 0.3908 |
| $\mathbf{R}^*_U = [6 \quad 0 \quad 0 \quad 3 \quad 1]$ | 1.2360 | 1.2142 |

$\mathbf{R}^*_{PW}$ was obtained with the total power set as the power consumed by 5 sensors when each sensor uses $R_i = 2$ bits.

The test results for $\mathbf{R}^*_{PW}$ and several uniform rate allocations $\mathbf{R}^U$'s are provided for comparison in Table 2.5. It can be seen that the sensors (sensors 2,4 and 5) closer to $\mathbf{x}_f$ will be assigned higher rate and sensor 3 will be allocated lower rate since it would provide redundant information along with sensor 5. Note that significant power savings (over 60%) can be achieved by the rate allocation, $\mathbf{R}^*_{PW}$ as compared with $\mathbf{R}^U = [5 \quad 5 \quad 5 \quad 5 \quad 5]$. Obviously, the optimal rate allocation $\mathbf{R}^* = [4 \quad 3 \quad 0 \quad 3 \quad 0]$ obtained under equal power assumption ($C_i$ =constant) is no longer the optimal one for this rate allocation problem.

#### 2.6.2.4 Performance analysis – comparison with uniform rate allocation

Figure 2.6 demonstrates the benefits of our optimal rate allocation, $\mathbf{R}^*$, as compared to uniform rate allocation, $\mathbf{R}^U = (R_1 = \frac{R_T}{M}, ..., R_M = \frac{R_T}{M})$. For the sensor configuration in Figure 2.3 the total rate, $R_T$, is varied from 10 to 20 bits. For each $R_T$, $\mathbf{R}^*$ is obtained

Table 2.5: Localization error ($m^2$) for various sets of rate allocations where $\mathbf{R}^*_{PW}$ was obtained by GBFOS using EDQ given $P = \sum_i C_i R_i = \sum_i 2C_i$. Localization error is given by $E(\| \mathbf{x} - \hat{\mathbf{x}} \|^2)$.

| Sets of rate allocations | EDQ | Power Consumption |
|---|---|---|
| $\mathbf{R}^*_{PW} = [0 \quad 6 \quad 0 \quad 4 \quad 3]$ | 0.0155 | 68.5841 |
| $\mathbf{R}^* = [4 \quad 3 \quad 0 \quad 3 \quad 0]$ | 0.1533 | 78.6355 |
| $\mathbf{R}^U = [2 \quad 2 \quad 2 \quad 2 \quad 2]$ | 0.6199 | 71.9401 |
| $\mathbf{R}^U = [3 \quad 3 \quad 3 \quad 3 \quad 3]$ | 0.1547 | 107.9101 |
| $\mathbf{R}^U = [5 \quad 5 \quad 5 \quad 5 \quad 5]$ | 0.0204 | 179.8502 |

by rate allocation process using EDQs and then the LSQs are designed for each $\mathbf{R}^*$ for comparison. The two rate allocations $(\mathbf{R}^*, \mathbf{R}^U)$ were tested using a test set of 2000 source locations with two measurement noise scenarios $\sigma_i = 0$ and $\sigma_i = 0.05$. In Figure 2.6, we compare performance under both EDQ and LSQ for both uniform and optimized rate allocation ($\mathbf{R}^U$ and $\mathbf{R}^*$ respectively). This experiment shows that significant gains can be achieved by using optimal rate allocation even when there is measurement noise. Note that the gain achieved by using optimal bit allocation (rather than uniform bit allocation) is greater for EDQ. This can be explained by the fact that EDQ does not use sensor location information when the bit allocation is uniform, whereas LSQ does incorporate location information even in the uniform case. Thus more gain can be expected for EDQ because the optimal bit allocation allows sensor location to be used to improve performance. We also note that EDQs with optimized allocation in fact provide better localization accuracy than LSQs with uniform allocation. This suggests that using the bit allocation process to improve performance could be a good design strategy, as it allows competitive performance to be achieved even with simple quantizers such as EDQ.

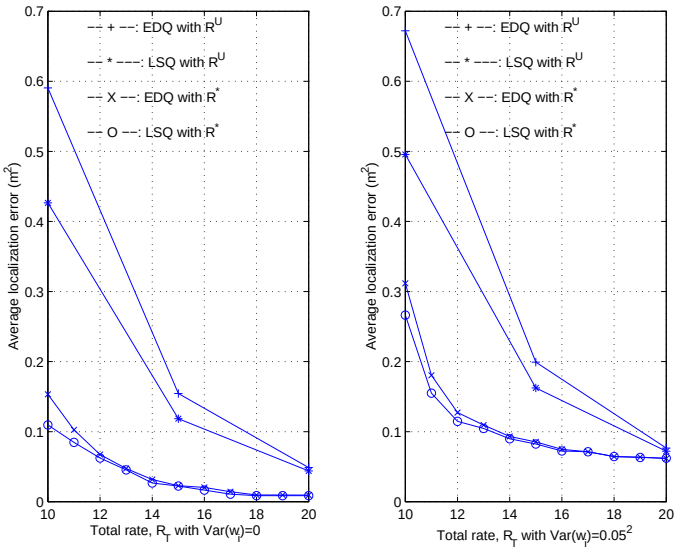


Figure 2.6: Comparison of optimal rate allocation, $\mathbf{R}^*$ with uniform rate allocation $\mathbf{R}^U$. LSQs are designed for each $\mathbf{R}^*$ and $\mathbf{R}^U$. 4 curves are plotted for comparison. For example, "EDQ (or LSQ) with $\mathbf{R}^U$ (or $\mathbf{R}^*$)" indicates the curve of localization error computed when each sensor uses EDQ (or LSQ) designed for $\mathbf{R} = \mathbf{R}^U$ (or $\mathbf{R}^*$).

A comparison between standard uniform quantization with uniform bit allocation (which would be a straightforward design for this system) and LSQ with optimal bit allocation is also useful. As can be seen in Figure 2.7 a significant gain (over 60% rate savings) can be achieved by the rate allocation optimized with LSQs.

Finally, our rate allocation was evaluated for different sensor configurations where 5 sensors are randomly deployed in $10 \times 10m^2$ sensor field. In the experiments, 100 different sensor configurations are generated and for each configuration, rate allocation using EDQ is performed to obtain $\mathbf{R}^*$. The localization error is averaged over 100 configurations and compared with that for $\mathbf{R}^U$. Figure 2.8 shows that the rate allocation is more important than quantizer design alone for obtaining good localization accuracy.

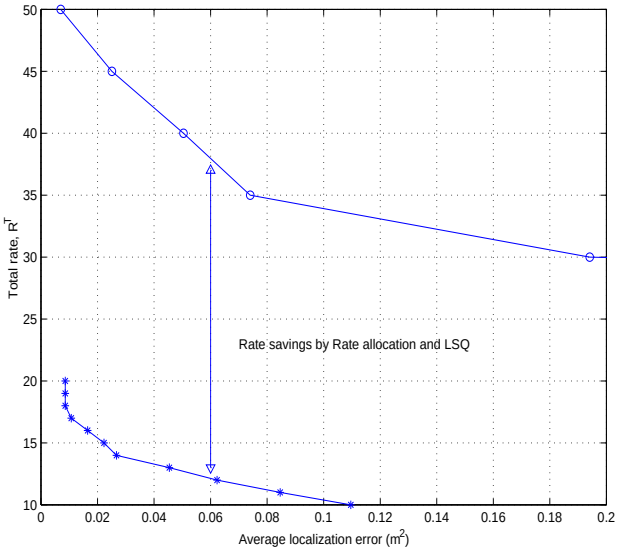


Figure 2.7: Gain in rate savings achieved by our optimal rate allocation, $\mathbf{R}^*$ using LSQs as compared with trivial solution where each sensor uses uniform quantizers of the same rate.

#### 2.6.2.5 Discussion

From our rate allocation experiments we observe first that significant gains can be achieved by assigning different rates to sensors at different locations. Second, we also note that in regions where sensors are clustered each sensor uses a smaller number of bits, while sensors that are further apart are allocated more bits. Third, EDQ is a useful practical design due to its simplicity, implying that some geometry-driven quantizers can be similarly introduced in real situations. Finally, noting the close relationship between sensor locations and their relative rates (equivalently, weights) assigned, we can develop simple and powerful algorithms that should use solely geometry information. For example, the relative distances between sensors or directional information could be effectively used for applications such as sensor networks that require a simple computing process and/or low power consumption.

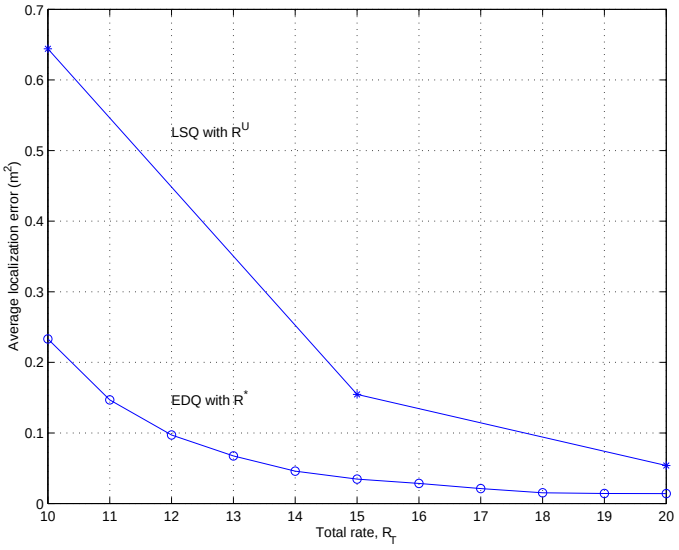


Figure 2.8: Evaluation of optimal rate allocation for many different sensor configurations. Localization error is averaged over 100 sensor configurations for two different rate allocations: $\mathbf{R}^U$ and $\mathbf{R}^*$.

## 2.7 Conclusion

In this chapter, we addressed the quantizer design and rate allocation problems for source localization. We proposed an iterative design algorithm that allows us to reduce the localization error for quantizer design. We showed that we can obtain the optimal rate allocation by applying the well known GBFOS algorithm along with LSQ. To overcome the complexity due to the rate allocation process, we introduced a simple quantizer, EDQ.

As future work, we are considering new algorithms for rate allocation with low complexity so that they can be applied to large-scale sensor networks. We will also study the case of multiple sources and another application (e.g., vehicle tracking) which requires rate allocation. In addition, since the channel between each sensor and the fusion node is not perfect, this should be taken into account for future research.

# Chapter 3

# Localization Algorithm based on Quantized data

## 3.1 Introduction

Source localization based on quantized acoustic sensor readings has been discussed in Section 2.5.1 for the case of no measurement noise and known source signal energy. In this chapter, we extend the work and propose a distributed source localization algorithm under more challenging conditions, including measurement noise as well as unknown source signal energy. If there is no measurement noise and the source signal energy is known, the only source location uncertainty is due to quantization. Because the source signal energy is known, each quantized reading can be mapped to a region in the sensor field, such that the shape of the region depends on the characteristics of the sensor.

For the case of an acoustic sensor that provides no directional information, the region corresponding to one quantized reading takes the form of a "ring" centered at the sensor location (see Figure 2.1 in Section 2.5.1). Since the measurements are assumed to be noiseless the source can be located by intersecting the regions corresponding to each sensor. A vector of measurements (one per sensor) will correspond to a unique location

and, after quantization, there will be a unique (non-empty) intersection region that will contain the position of the source. In this scenario efficient quantizer designs aim at minimizing the average area of all admissible intersections (see Chapter 2 and [16]).

Clearly, localization becomes more difficult when there is non-negligible measurement noise and/or the source signal energy is not known. In particular, some vector readings may lead to empty intersection regions and a given source location can produce different quantized measurements, depending on noise conditions.

To address these problems we use a probabilistic formulation, where we estimate the probability that each candidate location may have produced a given vector reading. In this context, we first formulate the source localization problem as minimum mean square error (MMSE) estimation problem; this approach generally has significant computational complexity, especially for the non-Gaussian case[1] we are addressing in this chapter [14].

We show that the complexity can be significantly reduced by taking into account the quantization effect and the distributed property of the quantized data while maintaining good localization accuracy. Based on this, first, under the assumption of known source signal energy, we propose a distributed algorithm based on the maximum a posteriori (MAP) criterion. We also show that for the case of unknown source signal energy, good localization performance can be achieved by using a weighted average of the estimates obtained by our proposed localization algorithm under different source energy assumptions.

[1] In the acoustic sensor case, the received quantized data and the source location are not jointly Gaussian.

## 3.2 Problem Formulation

Recall the sensing scenario described in Section 2.2 where we discussed the localization problem considered when the source signal energy, $a$, is known and there is no measurement noise ($w_i = 0$ in (2.1)). Consider now the case where there is measurement noise and/or the source signal energy is unknown. There is no guarantee that the intersection constructed from quantized readings (see Figure 2.1) is always nonempty. Furthermore, the source location, $\mathbf{x}$ might be located outside the intersection if it is nonempty. Thus, we need to consider all possible quantized values that a given source location can produce with the measurement noise and unknown energy.

Assuming the statistics of the measurement noise $w_i$ are known, we can formulate the source localization problem as MMSE estimation problem as follows:

$$\begin{aligned} \hat{\mathbf{x}} &= E(\mathbf{x}|\mathbf{Q_r}) = \int_{\mathbf{x}\in S} \mathbf{x} p(\mathbf{x}|\mathbf{Q_r}) d\mathbf{x} && (3.1) \\ &= \int_{\mathbf{x}\in S} \mathbf{x} p(\mathbf{Q_r}|\mathbf{x}) p(\mathbf{x}) / p(\mathbf{Q_r}) d\mathbf{x} && (3.2) \\ &= \frac{\int_{\mathbf{x}\in S} \mathbf{x} [\prod_{i=1}^{M} \int_{z_i \in Q_i} p(z_i|\mathbf{x}) dz_i] p(\mathbf{x}) d\mathbf{x}}{p(\mathbf{Q_r})} && (3.3) \end{aligned}$$

where $p(\mathbf{Q_r}) = \int_{\mathbf{x}\in S} [\prod_{i=1}^{M} \int_{z_i \in Q_i} p(z_i|\mathbf{x}) dz_i] p(\mathbf{x}) d\mathbf{x}$. The conditional probability $p(z_i|\mathbf{x}), i = 1, ..., M$ in (3.3) can be obtained by the sensor model in (2.1) and knowledge of $a$ (e.g., a pdf of $a$) as follows:

$$p(z_i|\mathbf{x}) = \int_a p(z_i|\mathbf{x}, a) p(a) da \tag{3.4}$$

where $p(z_i|\mathbf{x}, a)$ is a normal distribution with mean $g_i \frac{a}{\|\mathbf{x}-\mathbf{x}_i\|^\alpha}$ and variance $\sigma_i^2$. Note that in computing $p(z_i|\mathbf{x}, a)$, it is assumed that the measurement noise $w_i$ is normal distributed

with zero mean and variance, $\sigma_i^2$. Clearly, if the conditional probability $p(z_i|\mathbf{x})$ and $p(\mathbf{x})$ are given, the MMSE estimator $\hat{\mathbf{x}}$ can be obtained using (3.3). It can be noted that although the MMSE estimation provides an optimal estimate of the source location, it would require very large computational complexity to perform the integration over the sensor field $S$ and would also require knowledge of the prior distributions, such as $p(\mathbf{x})$ and $p(a)$. In this chapter, we use an uninformative or uniform prior distribution whenever there is ignorance about the parameters to be estimated, since this allows us to obtain an a posteriori distribution that will be approximately proportional to the likelihood. The uninformative prior has the added advantage of keeping subsequent computations relatively simple.

Now, in the following sections, we develop our localization algorithm, which is shown to achieve good performance with reasonable complexity as compared with the MMSE estimation.

## 3.3 Localization Algorithm based on Maximum A Posteriori (MAP) Criterion: Known Signal Energy Case

First, we assume that the source signal energy $a$ is known at the fusion node when the localization is performed. The case of unknown signal energy is treated in Section 3.5. Even when there is no measurement noise ($w_i = 0$ in (2.1)), there still exists some degree of uncertainty on the source location, due to the quantization. That is, the best thing we can do for localization based on quantized measurements would be to identify a region where the source is located. Thus, when quantization is used, we need candidate regions

where the source might be, rather than all candidate source locations. This is helpful in reducing the complexity of estimating source locations.

Since each observed $M$-tuple corresponds to a different spatial region in the noiseless case, we can partition the source field $S$ into $|S_Q^f|$ regions where $S_Q^f$ is the set of the $M$-tuples that can be generated in a noise-free environment. This can be written as follows:

$$S_Q^f = \{(Q_1, ..., Q_M) | g_i \frac{a}{\|\mathbf{x} - \mathbf{x}_i\|^\alpha} \in Q_i, i = 1, ..., M \quad \mathbf{x} \in S\} \tag{3.5}$$

For the $j$-th element, $\mathbf{Q^j}$ in $S_Q^f$, we can construct a corresponding region, $A^j$ in $S$ as follows:

$$A^j = \bigcap_{i=i}^{M} A_i, \quad A_i = \{\mathbf{x} | g_i \frac{a}{\|\mathbf{x} - \mathbf{x}_i\|^\alpha} \in Q_i^j, \quad \mathbf{x} \in S\} \tag{3.6}$$

where $\mathbf{Q^j} = (Q_1^j, ..., Q_M^j)$. Clearly, there is one to one correspondence between each region $A^j$ and each $\mathbf{Q}^j$ in $S_Q^f$.

In what follows, we first consider how to select the region that maximizes the probability $Pr[A^j|\mathbf{Q_r}], \quad \forall j$ where the received $M$-tuple, $\mathbf{Q_r}$, is typically noise corrupted and thus $\mathbf{Q_r}$ may not belong to $S_Q^f$. Then, we estimate the source location as the centroid of the region we selected. Based on this, the localization algorithm can be formulated as follows:

Let $H_j$ be the $j$-th hypothesis, corresponding to the $j$-th region, $A^j$, which can be obtained using the $j$-th $M$-tuple, $\mathbf{Q^j}$, in the set $S_Q^f$. Now, we seek to identify the hypothesis, $H^*$, that maximizes the probability $Pr[H_j|\mathbf{Q_r}], \forall j$.

$$
\begin{aligned}
H^* &= \arg\max_j p(H_j|\mathbf{Q_r}) \quad j = 1, ..., |S_Q^f| \\
&= \arg\max_j p(A^j|\mathbf{Q_r}) \\
&= \arg\max_j p(\mathbf{Q_r}|\mathbf{x} \in A^j)p_j, \qquad p_j = p(\mathbf{x} \in A^j) \\
&= \arg\max_j \prod_{i=1}^{M} p(Q_i|\mathbf{x} \in A^j)p_j,
\end{aligned} \tag{3.7}
$$

where the conditional probability, $p(Q_i|\mathbf{x} \in A^j)$ is computed in the following way:

$$
\begin{aligned}
& p(Q_i|\mathbf{x} \in A^j) = p(\mu_i(\mathbf{x}) + w_i \in Q_i|\mathbf{x} \in A^j) \\
= \;& p(Q_{i,l} - \mu_i(\mathbf{x}) \leq w_i \leq Q_{i,h} - \mu_i(\mathbf{x})|\mathbf{x} \in A^j) \\
= \;& \int_{\mathbf{x} \in A^j} [\Phi(\frac{Q_{i,h} - \mu_i(\mathbf{x})}{\sigma_i}) - \Phi(\frac{Q_{i,l} - \mu_i(\mathbf{x})}{\sigma_i})] p_j(\mathbf{x}) d\mathbf{x},
\end{aligned} \tag{3.8}
$$

where $\mu_i(\mathbf{x}) = g_i \frac{a}{\|\mathbf{x}-\mathbf{x}_i\|^\alpha}$ and $p_j(\mathbf{x}) = p(\mathbf{x}|\mathbf{x} \in A^j)$. Here $\Phi(.)$ is the cdf for the normal distribution, $N(0, 1)$. Once $H^*$ is obtained, the source estimate $\hat{\mathbf{x}}$ is computed by $E(\mathbf{x}|H^*) = E(\mathbf{x}|\mathbf{x} \in A^*)$.

It should be noticed that the proposed algorithm can be applied regardless of the sensor types, since each set of quantized sensor readings would generate a unique intersection under the assumption of no measurement noise. That is, we can obtain $H^*$ in (3.7) by replacing $g_i \frac{a}{\|\mathbf{x}-\mathbf{x}_i\|^\alpha}$ in (3.5) and (3.6) with the sensor model employed at each sensor.

## 3.4 Implementation of Proposed Algorithm

While the computational complexity of our MAP-based localization as described by (3.7) is lower than that for the MMSE estimation, the integration of (3.8) has to be performed for each hypothesis, which is computationally complex. To make it practical, the localization algorithm needs some modification so that the complexity due to $|S_Q^f|$ integrations per $\mathbf{Q_r}$ should be significantly reduced, so that only a few integrations need to be performed.

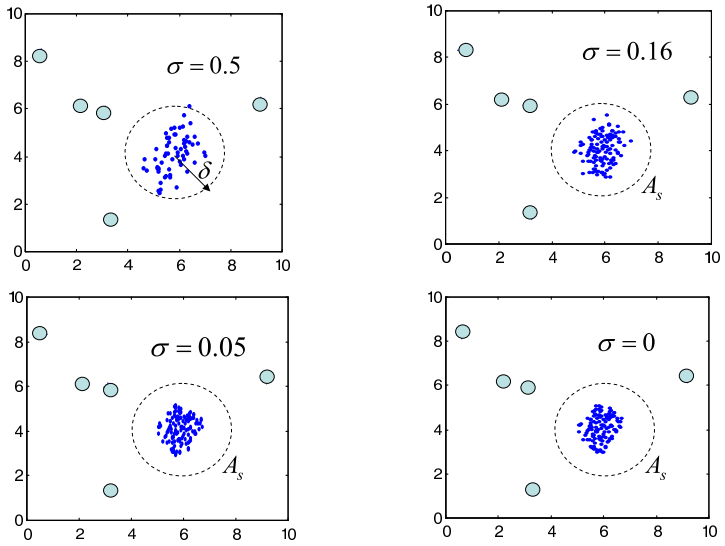


Figure 3.1: Source locations that generate the given $\mathbf{Q_r}$ for each variance ($\sigma = 0, 0.05, 0.16, 0.5$) are plotted. 5 sensors (marked as $\circ$) are employed in a sensor field $10 \times 10m^2$ and each sensor uses a 2-bit quantizer.

It should be observed that, even in the noisy case, if the source is in $A^j$ corresponding to $\mathbf{Q^j} \in S_Q^f$, the corresponding quantized vector reading is likely to be $\mathbf{Q^j}$. Clearly, the

number of source locations belonging to $A^j$ that produce $\mathbf{Q^j}$ would be larger at higher SNR.

Figure 3.1 demonstrates this observation: in this experiment, a test set of 5000 source locations is generated for each $\sigma = 0, 0.05, 0.16, 0.5$ and only source locations generating the given $\mathbf{Q_r}$ are plotted for each test set. Based on this observation, it would be possible to construct a set, $A_s(\subset S)$ such that $p(\mathbf{x} \in A_s|\mathbf{Q_r}) \approx 1$, allowing us to consider only the hypotheses (or regions) that belong to the set $A_s$, leading to a reduction in the number of the hypotheses that have to be evaluated for the MAP-based localization.

This set can be constructed by noting that given a source location $\mathbf{x}$, and the corresponding noisy $M$-tuple $\mathbf{Q_r}$, it is be very likely that $p(\mathbf{x} \in A^i|\mathbf{Q_r}) > p(\mathbf{x} \in A^j|\mathbf{Q_r})$ as long as $p(\hat{\mathbf{x}}_i|\mathbf{Q_r}) \gg p(\hat{\mathbf{x}}_j|\mathbf{Q_r})$, where $\hat{\mathbf{x}}_j$ is the centroid of the set $A^j$. In other words, we first choose the most likely centroid, say $\hat{\mathbf{x}}_c$ given $\mathbf{Q_r}$ and construct $A_s(\delta) = \{\mathbf{x}| \parallel \mathbf{x} - \hat{\mathbf{x}}_c \parallel < \delta, \mathbf{x} \in S\}$ such that we can obtain the set $A_s(\delta)$ satisfying $P(\mathbf{x} \in A_s(\delta)) \approx 1$, with a reasonable choice of $\delta$. Clearly, the smaller the $\delta$ we choose, the more reduction in computational complexity we can achieve at the cost of increased localization error. This consideration leads us to a practical implementation of the algorithm as follows:

1) Initial search (coarse search):

$$\begin{aligned}
\hat{\mathbf{x}}_c &= \arg\max_j p(\hat{\mathbf{x}}_j|\mathbf{Q_r}), \text{where} \quad \hat{\mathbf{x}}_j = E(\mathbf{x}|\mathbf{x} \in A^j) \\
&= \arg\max_j p(\mathbf{Q_r}|\hat{\mathbf{x}}_j)p_j \\
&= \arg\max_j \prod_{i=1}^{M} [\Phi(\frac{Q_{i,h} - \mu_i(\hat{\mathbf{x}}_j)}{\sigma_i}) - \Phi(\frac{Q_{i,l} - \mu_i(\hat{\mathbf{x}}_j)}{\sigma_i})]p_j
\end{aligned}$$

2) Refined search:

Once $\hat{\mathbf{x}}_c$ is obtained, we can construct the set $A_s(\delta) = \bigcup_{k=1}^{K} A^k$ (clearly, $A_s \in S$) such that $\| \hat{\mathbf{x}}_c - \hat{\mathbf{x}}_k \| < \delta, \quad \forall k = 1, ..., K$ where $\hat{\mathbf{x}}_k = E(\mathbf{x}|\mathbf{x} \in A^k)$. Now, we can compute $H^*$ using $K$ hypotheses as follows:

$$H^* = \arg\max_k p(A^k|\mathbf{Q_r}), \quad k = 1, ..., K \tag{3.9}$$

$$= \arg\max_k p(\mathbf{Q_r}|\mathbf{x} \in A^k)p_k, \quad p_k = p(\mathbf{x} \in A^k) \tag{3.10}$$

$$= \arg\max_k \prod_{i=1}^{M} p(Q_i|\mathbf{x} \in A^k)p_k \tag{3.11}$$

Notice that $K$ takes a small value ($\ll |S_Q^f|$) with a good choice[2] of $\delta$.

## 3.5 Unknown Signal Energy Case

So far, we assumed that the source signal energy, $a$, is known to the fusion node where the localization is performed based on quantized data. However, the source energy is generally unknown and should be also estimated along with the source location. A possible solution would be to adopt the energy ratios-based source localization method proposed in [19] where the authors took ratios of the *unquantized* energy readings of a pair of sensors in the noise-free case to cancel out the energy, $a$, and formulated a nonlinear least square optimization problem. However, while the method shows good performance with low-complexity implementation for unquantized sensor readings and provides full robustness to unknown source energies, it would have some drawbacks when the sensor

[2]A good choice of $\delta$ depends upon the experimental settings, such as $M, R_i$, sensor models and other factors.

energy readings are quantized. This is because the fusion node has to obtain the energy ratios based on quantization intervals. This leads to larger range of possible values for the energy ratios and thus increased uncertainty about the source location.

In this section, we consider the localization problem with unknown energy as an extension of the estimation problem explained in the previous sections and we show that a good estimate of the source location can be represented by a weighted average of source estimates, each of which is obtained by the proposed algorithm in Section 3.3. With the unknown source signal energy $a$, termed a nuisance parameter [10], we can reformulate the MMSE estimation problem from Section 3.2 as follows:

$$\begin{aligned}
\hat{\mathbf{x}} &= E[\mathbf{x}|\mathbf{Q_r}] = \int_{\mathbf{x}\in S} \mathbf{x} p(\mathbf{x}|\mathbf{Q_r}) d\mathbf{x} && (3.12)\\
&= \int_{\mathbf{x}} \mathbf{x}[\int_a p(\mathbf{x}, a|\mathbf{Q_r}) da] d\mathbf{x} && (3.13)\\
&= \int_{\mathbf{x}} \mathbf{x}[\int_a p(\mathbf{x}|\mathbf{Q_r}, a) p(a|\mathbf{Q_r}) da] d\mathbf{x} && (3.14)\\
&= \int_a [\int_{\mathbf{x}} \mathbf{x} p(\mathbf{x}|\mathbf{Q_r}, a) d\mathbf{x}] p(a|\mathbf{Q_r}) da && (3.15)\\
&= \int_a \hat{\mathbf{x}}_{MMSE}(a) p(a|\mathbf{Q_r}) da && (3.16)\\
&\approx \int_a \hat{\mathbf{x}}_{prop}(a) p(a|\mathbf{Q_r}) da. && (3.17)
\end{aligned}$$

In (3.17), the MMSE estimate, $\hat{\mathbf{x}}_{MMSE}$ given by (3.3) is replaced by the estimate $\hat{\mathbf{x}}_{prop}$ obtained by the localization algorithm proposed in Section 3.3. Note that computing $p(a|\mathbf{Q_r})$ can be complex:

$$p(a|\mathbf{Q_r}) = \int_{\mathbf{x}} p(\mathbf{x}, a|\mathbf{Q_r})d\mathbf{x} \tag{3.18}$$

$$\propto p(a) \int_{\mathbf{x}} p(\mathbf{Q_r}|\mathbf{x}, a)p(\mathbf{x})d\mathbf{x}. \tag{3.19}$$

In order to reduce the complexity of computing (3.19), we further make the following approximations:

1. While the source signal energy can take continuous values in a predetermined interval $[a_{min} \quad a_{max}]$, we consider only discrete energy values, since small variations in signal energy have a small impact on localization accuracy (see Figure 3.2). Based on this, (3.17) can be written as

$$\hat{\mathbf{x}} \approx \int_a \hat{\mathbf{x}}_{prop}(a)p(a|\mathbf{Q_r})da \tag{3.20}$$

$$\approx \sum_{a_k}^{N} \hat{\mathbf{x}}_{prop}(a_k)p(a_k|\mathbf{Q_r}) \tag{3.21}$$

$$= \sum_{a_k}^{N} \frac{\hat{\mathbf{x}}_{prop}(a_k)W_k}{\sum W_i} \tag{3.22}$$

   where $N$ is the number of discrete energy values used and $W_k$ is the $k$-th weight factor which can be rewritten as

$$W_k = p(a_k) \int_{\mathbf{x}\in S} p(\mathbf{Q_r}|\mathbf{x}, a_k)p(\mathbf{x})d\mathbf{x}. \tag{3.23}$$

2. Some signal energy values are bound to be less likely than others (for example, a particular energy value can lead to a non empty intersection of quantization regions,

while under other energy values the intersections may be empty). Thus, there will be some dominant weights in (3.23) and if we compute the weights first, we only need to perform the localization algorithm for those weights that are sufficiently large. Refer to Figure 3.2, which illustrates that a few weights (3 or 4) are sufficiently large while others can be ignored. Thus, we can approximate (3.22) by $\sum_{l=1}^{L} \frac{\hat{\mathbf{x}}_{prop}(a_l)W_l}{\sum_i^L W_i}$ where it is assumed that the set of weights, $\{W_k\}_{k=1}^{N}$ is arranged such that $W_1 \geq W_2 \geq ... \geq W_L \geq ... \geq W_N$.

3. Finally, since we can construct a set $A_s(\delta_w, a_k)$ using the coarse search described in Section 3.4, this set can also be used to compute the weights given by (3.23):

$$W_l \approx p(a_l) \int_{\mathbf{x} \in A_s(\delta_w, a_l)} p(\mathbf{Q_r}|\mathbf{x}, a_l) p(\mathbf{x}) d\mathbf{x} \tag{3.24}$$

Clearly, there will be some trade-offs between the computational complexity and the localization performance and this can be controlled by adjusting parameters such as $N, L$, and $\delta_w$.

## 3.6 Simulation Results

We consider a sensor network of M sensors deployed randomly in a $10 \times 10m^2$ sensor field ($M = 3, 4$ and 5 in our experiments). Each sensor measures an acoustic source energy based on the energy decay model in (2.1), quantizes it using a quantizer designed by the algorithm in Chapter 2 and sends it to a fusion node where localization is performed

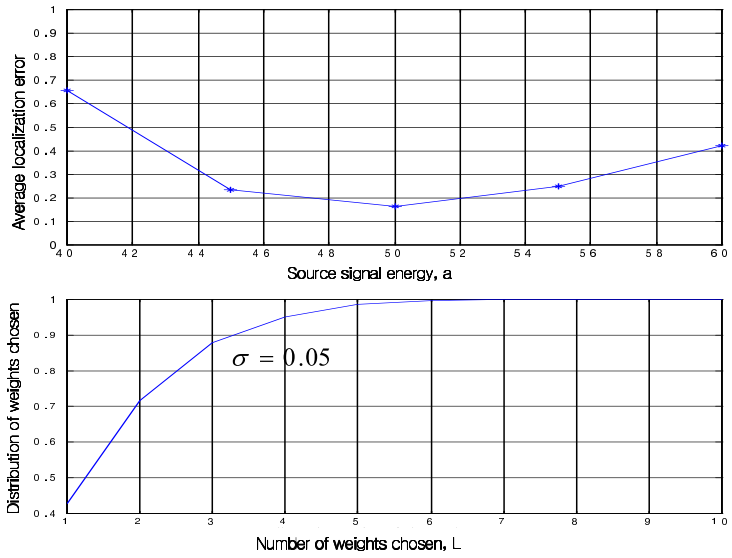


Figure 3.2: Localization accuracy of proposed algorithm under source signal energy mismatch (top). In this experiment, a test set of 2000 source locations is generated for each source signal energy ($a = 40, 45, ..., 55, 60$). Localization is performed by the proposed algorithm in Section 3.4 using $a = 50$ and $\delta = 1m$. Distribution of weights vs. Number of weights chosen, $L$. (bottom) ($\frac{\sum_l^L W_l}{\sum_k^N W_k}$ vs. $L$). A test set of 2000 source locations is generated and N=10 weights are computed for each source location.

using our proposed localization algorithms. Note that the measurement noise is assumed to be normal distributed with zero mean and a variance of $\sigma^2$.

### 3.6.1 Case of known signal energy

First, assuming $a$ is known, the distributed localization algorithm proposed in Section 3.4 is tested using a test set of 2000 source locations generated with $p(\mathbf{x})$ modeled by a uniform distribution for each ($\sigma$,M) pair, where $\sigma$ varies from 0 to 0.5 and M=3,4 and 5. In Figure 3.3 the proposed algorithm is compared to the MMSE estimation given by (3.3) since the latter gives us a good lower bound for testing our localization algorithm.

Note that we choose $\delta = 1m$ in our algorithm. From Figure 3.3, it can be said that our algorithm provides localization accuracy close to that for MMSE estimation, especially when $\sigma < 0.16$.

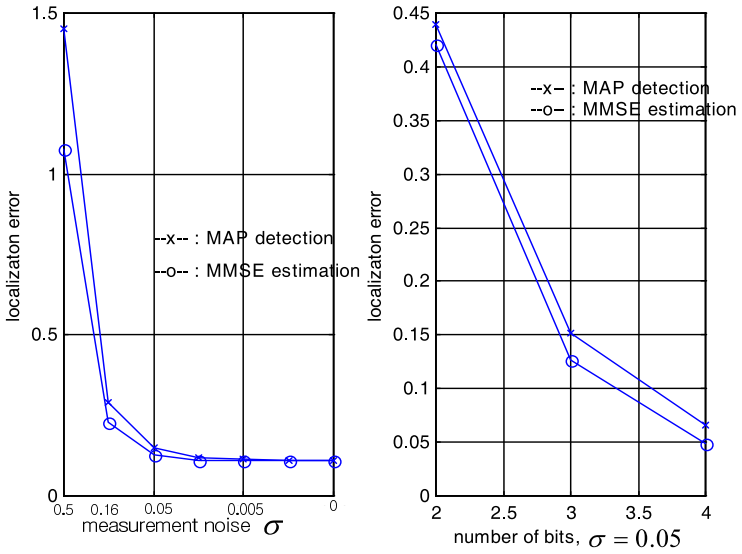


Figure 3.3: Localization algorithms based on MMSE and MAP criterion are tested when $\sigma$ varies from 0.5 to 0 with $R_i = 3$ (left) and when $R_i = 3, 4$ and 5 with $\sigma = 0.05$ (right) and $\delta = 1m$ respectively. $w_i \sim N(0, \sigma^2)$.

### 3.6.2 Case of unknown signal energy

Our distributed localization algorithm for the unknown source signal energy case of Section 3.5 is tested and compared with the MMSE estimator and the energy ratio based method and also evaluated under various types of mismatches. In applying the localization algorithm, prior distributions for $p(\mathbf{x})$ and $p(a)$ are assumed to be uniform over $\mathbf{x} \in S$ and $a \in [a_{min} \quad a_{max}] = [0 \quad 100]$, respectively and the parameters are set as $N = 10, a_k \in \{10, 20, ..., 100\}, L = 3, \delta_w = 1m, \alpha = 2, g_i = 1$.

In Figure 3.4, the interval $[a_{min} \quad a_{max}]$ is divided into 8 subintervals, namely [20 30],...,[90 100], and for each subinterval, a test set of 2000 source locations with the source signal energy randomly drawn from the subinterval is generated with $\sigma = 0.05$. Clearly, as we mentioned in Section 3.5, the energy ratio-based method provides worse localization accuracy than our proposed algorithm.

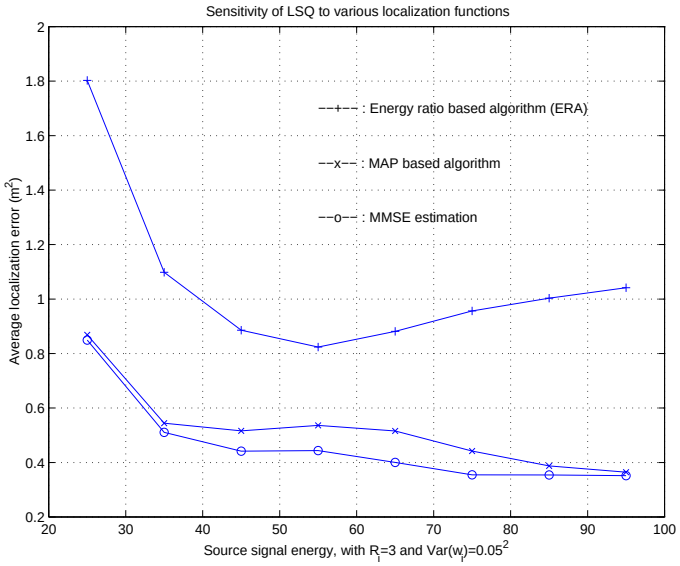


Figure 3.4: Localization algorithms based on MMSE estimation, MAP criterion and energy ratios are tested by varying source signal energy $a$ from 20 to 100. We set $N = 10, L = 3$, and $\delta_w = 1m$ in our algorithm. In this experiment, a test set with $M = 5, R_i = 3$ is generated with uniform distribution of source locations for each signal energy and the measurement noise is modeled by a normal distribution with zero mean and $\sigma = 0.05$.

### 3.6.3 Sensitivity to parameter mismatches

Table 3.1 shows results when one of the parameters is randomly perturbed: that is, the actual value of $\alpha$ in generating a test set is randomly drawn from the interval $[2-\Delta\alpha, \quad 2+\Delta\alpha]$ with $\Delta\alpha = 0, 0.1, ..., 0.4$ and the actual gain also drawn randomly from a uniform distribution $[1-\Delta g \quad 1+\Delta g]$. Similarly, each sensor location $(x, y)$ is randomly generated

from $[x-\Delta x \quad x+\Delta x]$ and $[y-\Delta y \quad y+\Delta y]$, respectively with $\Delta x = \Delta y = 0, 0.1, ..., 0.4$. In addition, a test set of 2000 source locations with normal distribution with mean $(5, 5)$ and variance $(\sigma_x^2, \sigma_y^2)$ is generated for $\sigma_x = \sigma_y = 1, 1.5, 2, 2.5$ and 3. From the results in Table 3.1, it can be said that small perturbations do not result in significant degradation in localization accuracy.

| $\Delta\alpha$ | 0 | 0.1 | 0.2 | 0.3 | 0.4 |
|---|---|---|---|---|---|
| LE (MAP) | 0.5319 | 0.7360 | 1.4643 | 2.2653 | 3.6998 |
| LE (ERA) | 0.8886 | 1.1402 | 1.8658 | 2.7042 | 3.6696 |
| $\Delta g_i$ | 0 | 0.1 | 0.2 | 0.3 | 0.4 |
| LE (MAP) | 0.5414 | 0.6293 | 0.8201 | 1.1606 | 1.6215 |
| LE (ERA) | 0.8980 | 0.9695 | 1.2012 | 1.6407 | 2.0873 |
| $(\Delta x, \Delta y)$ | 0 | 0.1 | 0.2 | 0.3 | 0.4 |
| LE (MAP) | 0.5414 | 0.5380 | 0.5836 | 0.6242 | 0.7176 |
| LE (ERA) | 0.8980 | 0.8900 | 0.9167 | 1.0074 | 1.0760 |
| $(\sigma_x, \sigma_y)$ | 1 | 1.5 | 2 | 2.5 | 3 |
| LE (MAP) | 0.2710 | 0.3554 | 0.4806 | 0.8992 | 1.7617 |
| LE (ERA) | 0.8879 | 0.9233 | 0.9732 | 1.4556 | 2.2024 |

Table 3.1: Localization error (LE) $(m^2)$ of MAP algorithm compared to energy ratios based algorithm (ERA) under various mismatches. In each experiment, a test set is generated with $M = 5$ and $\sigma = 0.05$ and one of the parameters is varied. Localization error (LE) $(m^2)$ is computed by $E(\| \mathbf{x} - \hat{\mathbf{x}} \|^2)$ using $\alpha = 2, g_i = 1, R_i = 3$ and uniform distribution of $p(\mathbf{x})$.

### 3.6.4 Performance analysis in a larger sensor network

Our MAP-based localization algorithm was also tested and compared with ERA in a larger sensor network $20 \times 20m^2$ where the number of sensors is $M = 12, 16, 20$. For each $M$, a test set of 4000 samples was generated using uniform priors for $p(\mathbf{x}), p(a)$ and normal measurement noise with $\sigma = 0.05$. Our proposed algorithm still shows better localization accuracy than the energy-ratios based algorithm (ERA) in larger sensor networks.

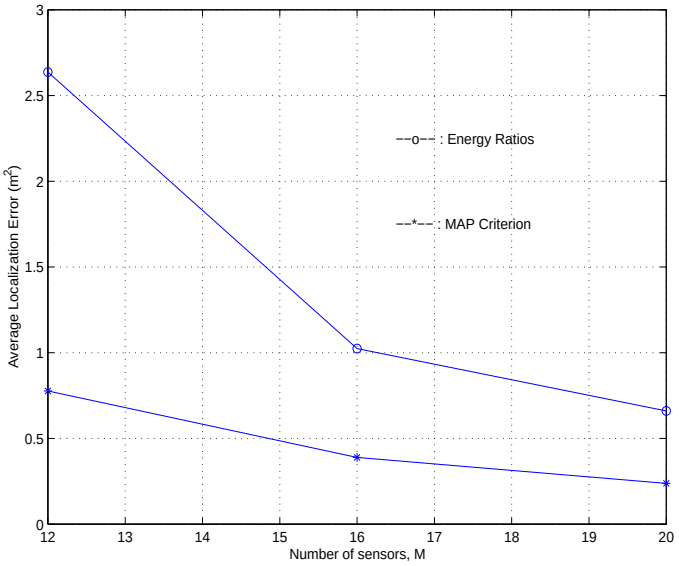


Figure 3.5: Localization algorithms based on MAP criterion and energy ratios are tested in a larger sensor network by varying the number of sensors. The parameters are $N = 10, L = 3$ and $\delta_w = 1m$ in our algorithm. In this experiment, a test set of 4000 samples was generated for $M = 12, 16, 20$. Each sensor uses a 3 bit quantizer and the measurement noise is modeled by the normal distribution with zero mean and $\sigma = 0.05$.

## 3.7 Conclusion

In this chapter, we considered the source localization based on acoustic sensor readings and proposed a distributed localization algorithm based on MAP criterion. We showed that the complexity could be significantly reduced by taking into account the correlation of quantized data without much degradation of localization accuracy.

# Chapter 4

# Distributed Encoding Algorithm

## 4.1 Introduction

In the quantizer design proposed in Chapter 2, our algorithm seeks to reduce the localization error by adjusting the size of a "fixed" number of quantization bins at each node.[1] In this chapter, we consider a novel way of reducing the total number of bits transmitted to the fusion node while preserving localization performance. It is shown that this can be accomplished by exploiting properties of the combinations of quantization bins that can be transmitted by the nodes. The basic concept can be motivated as follows. Suppose that one of the nodes reduces the number of bins that are being used. This will cause a corresponding increase in uncertainty. However, the fusion node that receives information from all the nodes can often compensate for this uncertainty by using data from the other nodes as side information.

More specifically, in the context of source localization, since each source location leads to a set of quantized sensor measurements that correspond to a non-empty intersection, the fusion node will only receive those combinations of quantized measurements that

[1] Each node may employ one sensor or an array of sensors, depending on the applications.

correspond to real source locations. Obviously, this is true only in the noiseless case. The key observation in this chapter is that the number of real quantized vector observations is smaller than the *total* number of possible combinations of quantized values at the nodes. Thus, many arbitrary combinations of quantized readings at several nodes *cannot be produced* because the corresponding regions have an empty intersection. Therefore, there will still be some redundancy after quantization which we will seek to reduce in order to decrease overall transmission rate.

In this chapter, we consider a distributed encoding algorithm that achieves significant rate savings by merging selected quantization bins without affecting localization performance. This algorithm is designed for the case when there is no measurement noise but we also show that it can be applied with slight modification (at the expense of potential decoding errors) even when there is measurement noise.

The assumptions made in Section 2.2 still hold throughout this chapter. This chapter is organized as follows. The definitions which will be used to derive our algorithm are provided in Section 4.2. The motivation is explained in Section 4.3. In Section 4.4, we consider quantization schemes that can be used with the encoding at each node. An iterative encoding algorithm is proposed in Section 4.5. For a noisy situation, we consider the modified encoding algorithm in Section 4.6 and describe the decoding process and how to handle decoding errors in Section 4.7. In Section 4.8, we apply our encoding algorithm to the source localization system where an acoustic amplitude sensor model is employed. Simulation results are given in Section 4.9 and the conclusions are found in Section 4.10.

## 4.2 Definitions

Let $S_M = I_1 \times I_2 \times ... \times I_M$ be the cartesian product of the sets of quantization indices. $S_M$ contains $|S_M| = (\prod_i^M L_i)$ $M$-tuples representing all possible combinations of quantization indices. We denote $S_Q$ the subset of $S_M$ that contains all the quantization index combinations that can occur in a real system, i.e., all those generated as a source moves around the sensor field and produces readings at each node:

$$S_Q = \{(Q_1, ..., Q_M) | \ \exists \mathbf{x} \in S, Q_i = \alpha_i(z_i(\mathbf{x})), \ i = 1, \ldots, M\} \tag{4.1}$$

We denote $S_i^j$ the subset of $S_Q$ that contains all $M$-tuples in which the $i$-th node is assigned quantization bin $Q_i^j$:

$$S_i^j = \{(Q_1, ..., Q_M) \in S_Q | Q_i = j\}. \tag{4.2}$$

For a given $Q_i^j$ we can always construct the corresponding $S_i^j$ from $S_Q$. Note also that $S_i^j \subset S_Q$. Along with this, we denote $\overline{S_i^j}$, the set of $(M-1)$-tuples obtained from $M$-tuples in $S_i^j$, where only the quantization bins at positions other than position $i$ are stored. That is, if $(Q_1, ..., Q_M) = (a_1, ..., a_M) \in S_i^j$ then we have $(a_1, ..., a_{i-1}, a_{i+1}, ..., a_M) \in \overline{S_i^j}$. There is a one to one correspondence between the elements in $S_i^j$ and $\overline{S_i^j}$ so that $|S_i^j| = |\overline{S_i^j}|$.

## 4.3 Motivation: Identifiability

In this section, we assume that $Pr[(Q_1, ..., Q_M) \in S_Q] = 1$, i.e., only combinations of quantization indices belonging to $S_Q$ can occur and those combinations belonging to $S_M -$

$S_Q$, which lead to an empty intersection, never occur. These sets can be easily obtained when there is no measurement noise (i.e., $w_i = 0$) and no parameter mismatches. As discussed in the introduction, there will be elements in $S_M$ that are not in $S_Q$. Therefore, simple scalar quantization at each node would be inefficient because a standard scalar quantizer would allow us to represent any of the $M$-tuples in $S_M$, but $|S_M| \geq |S_Q|$. What we would like to determine now is a method such that independent quantization can still be performed at each node, while at the same time we reduce the redundancy inherent in allowing all the combinations in $S_M$ to be chosen. Note that, in general, determining that a specific quantizer assignment in $S_M$ does not belong to $S_Q$ requires having access to the whole vector, which obviously is not possible if quantization has to be performed independently at each node.

In our design we will look for quantization bins in a given node that can be "merged" without affecting localization. As will be discussed next, this is because the ambiguity created by the merger can be resolved once information obtained from the other nodes is taken into account. Note that this is the basic principle behind distributed source coding techniques: binning at the encoder, which can be disambiguated once side information is made available at the decoder [7, 8, 12] (in this case quantized values from other nodes).

Merging of bins results in bit rate savings because fewer quantization indices have to be transmitted. To quantify the bit rate savings we need to take into consideration that quantization indices will be entropy coded (in this chapter Huffman coding is used). Thus, when evaluating the possible merger of two bins, we will compute the probability of the merged bin as the sum of the probabilities of the merged bins. For example, suppose

that $Q_i^j$ and $Q_i^k$ are merged into $Q_i^{min(j,k)}$. Then we can construct the set $S_i^{min(j,k)}$ and compute the probability for the merged bin as follows:

$$S_i^{min(j,k)} = S_i^j \cup S_i^k \tag{4.3}$$

$$P_i^{min(j,k)} = P_i^j + P_i^k \tag{4.4}$$

where $P_i^j = \int_{A_i^j} p(\mathbf{x})d\mathbf{x}$, $p(\mathbf{x})$ is the pdf of the source position and $A_i^j$ is given by

$$A_i^j = \{\mathbf{x}|(Q_1 = \alpha_1(z_1(\mathbf{x})), ..., Q_M = \alpha_M(z_M(\mathbf{x}))) \in S_i^j\} \tag{4.5}$$

Suppose the encoder at node $i$ merges $Q_i^j$ and $Q_i^k$ into $Q_i^l$ with $l = min(j,k)$, and sends the corresponding index to the fusion node. The decoder will construct the set $S_i^l$ for the merged bin using (4.3) and then will try to determine which of the two merged bins ($Q_i^j$ or $Q_i^k$ in this case) actually occurred at node $i$. To do so, the decoder will use the information provided by the other nodes, i.e., the quantization indices $Q_m$ ($m \neq i$). Consider one particular source position $\mathbf{x} \in S$ for which node $i$ produces $Q_i^j$ and the remaining nodes produce a combination of $M-1$ quantization indices $\mathbf{Q} \in \overline{S_i^j}$. Then, for this $\mathbf{x}$ there would be no ambiguity at the decoder, even if bins $Q_i^j$ and $Q_i^k$ were to be merged, as long as $\mathbf{Q} \notin \overline{S_i^k}$. This follows because if $\mathbf{Q} \notin \overline{S_i^k}$ the decoder would be able to determine that only $Q_i^j$ is consistent with receiving $\mathbf{Q}$. With the notation adopted earlier this leads to the following definition:

**Definition 1** *$Q_i^j$ and $Q_i^k$ are identifiable, and therefore can be merged, iff $\overline{S_i^j} \cap \overline{S_i^k} = \emptyset$.*

The question that remains is how to merge identifiable bins in order to minimize the total rate used by the $M$ nodes to transmit their quantized observations.

## 4.4 Quantization Schemes

As mentioned in the previous section, there will be redundancy in M-tuples after quantization which can be eliminated by our merging technique. However, we can also attempt to reduce the redundancy during quantizer design before the encoding of the bins is performed. Thus, it would be worth considering the effect of selection of a given quantization scheme on system performance when the merging technique is employed. In this section, we consider three schemes as follows:

- Uniform quantizers

  Since they do not utilize any statistics about the sensor readings for quantizer design, there will be no reduction in redundancy by the quantization scheme. Thus only the merging technique plays a role in improving the system performance.

- Lloyd quantizers

  Using the statistics about the sensor reading, $z_i$ available at node $i$, the $i$-th quantizer is designed using the generalized Lloyd algorithm [29] with the cost function $|z_i - \hat{z}_i|^2$ which is minimized in an iterative fashion. Since each node consider only the information available to it during quantizer design, there will still exist much redundancy after quantization which the merging technique can attempt to reduce.

- LSQ proposed in Chapter 2

  While designing a quantizer at node $i$, we take into account the effect of sensor

readings at other nodes on the quantizer design by defining a new cost function, $J = \sum_i^M |z_i - \hat{z}_i|^2 + \lambda \|\mathbf{x} - \hat{\mathbf{x}}\|^2$ which will be minimized in an iterative manner. Since the correlation between sensor readings is exploited during quantizer design, LSQ along with our merging technique will show the best performance of all.

We will discuss the effect of quantization and encoding on the system performance based on experiments for an acoustic amplitude sensor system in Section 4.9.1.

## 4.5 Proposed Encoding Algorithm

In general there will be multiple pairs of identifiable quantization bins that can be merged. Often, all candidate identifiable pairs cannot be merged simultaneously, i.e., after a pair has been merged, other candidate pairs may become non identifiable. In what follows we propose algorithms to determine in a sequential manner which pairs should be merged.

In order to minimize the total rate, an optimal merging technique should attempt to reduce the overall entropy as much as possible, which can be achieved by (1) merging high probability bins together and (2) merging as many bins as possible. It can be observed that these two strategies cannot be pursued simultaneously. This is because high probability bins (under our assumption of uniform distribution of the source position) are large and thus merging large bins tends to result in fewer remaining merging choices (i.e., a larger number of identifiable bin pairs may become non-identifiable after two large identifiable bins have been merged). Conversely, a strategy that tries to maximize the number of merged bins will tend to merge many small bins, leading to less significant

reductions in overall entropy. In order to strike a balance between these two strategies we define a metric, $W_i^j$, attached to each quantization bin:

$$W_i^j = P_i^j - \gamma |S_i^j|, \tag{4.6}$$

where $\gamma \geq 0$. This is a weighted sum of the bin probability and the number of quantizer combinations that include $Q_i^j$. If $P_i^j$ is large this would be a good candidate bin for merging under criterion (1), whereas a small value of $|S_i^j|$ will indicate a good choice under criterion (2). In our proposed procedure, for a suitable value of $\gamma$, we will seek to prioritize the merging of those identifiable bins having largest total weighted metric. This will be repeated iteratively until there are no identifiable bins left.

The proposed *global merging algorithm* is summarized as follows:

**Step 1**: Set $F(i,j) = 0$, where $i = 1, ..., M; j = 1, ..., L_i$, indicating that none of the bins, $Q_i^j$, have been merged yet.

**Step 2**: Find $(a,b) = \arg\max_{(i,j)|F(i,j)=0}(W_i^j)$, i.e., we search over all the non-merged bins for the one with the largest metric $W_a^b$.

**Step 3**: Find $Q_a^c, c \neq b$ such that $W_a^c = \max_{j \neq b}(W_a^j)$, where the search for the maximum is done only over the bins identifiable with $Q_a^b$ at node $a$. If there are no bins identifiable with $Q_a^b$, set $F(a,b) = 1$, indicating the bin $Q_a^b$ is no longer involved in the merging process. If $F(i,j) = 1, \forall i,j$, stop; otherwise go to Step 2.

**Step 4**: Merge $Q_a^b$ and $Q_a^c$ to $Q_a^{\min(b,c)}$ with $S_a^{\min(b,c)} = S_a^b \cup S_a^c$. Set $F(a, \max(b,c)) = 1$.

Given M quantizers, we can construct the sets $S_i^j$, and the metric $W_i^j, \forall i,j$, perform the merging using the proposed algorithm and find the parameter $\gamma$ in (4.6) that minimizes

the total rate[2]. In the proposed algorithm, the search for the maximum of the metric is done for the bins of all nodes involved. However, different approaches can be considered for the search. These are explained as follows:

**Method** 1: *Complete sequential merging.* In this method, we process one node at a time in a specified order. For each node, we merge the maximum number of bins possible before proceeding to the next node. Merging decisions are not modified once made. Since we exhaust all possible mergers in each node, after scanning all the nodes no more additional mergers are possible.

**Method** 2: *Partial sequential merging.* In this method, we again process one node at a time in a specified order. For each node, among all possible bin mergers, the best one according to a criterion is chosen (the criterion could be entropy-based and for example, (4.6) is used in this thesis) and after the chosen bin is merged we proceed to the next node. This process is continued until no additional mergers are possible in any node. This may require multiple passes through the set of nodes.

These two methods can be easily implemented with minor modifications to our proposed algorithm. Notice that the final result of the proposed encoding algorithm will be $M$ merging tables, each of which has the information about which bins can be merged at each node in real operation. That is, each node will merge the quantization bins using the merging table stored at the node and will send the merged bin to the fusion node which then tries to determine which bin actually occurred via the decoding process using $M$ merging tables and $S_Q$.

[2]A heuristic method can be used to search $\gamma$. Clearly, $\gamma$ depends on the application.

### 4.5.1 Incremental Merging

The complexity of the above procedures is a function of the total number of quantization bins, and thus of the number of nodes involved. Thus, these approaches could potentially be complex for large sensor fields. We now show that incremental merging is possible, that is, we can start by performing the merging based on a subset of $N$ sensor nodes, $N < M$, and will be guaranteed that merging decisions that were valid when $N$ nodes were considered will remain valid when all $M$ nodes are taken into account.

To see this, suppose that $Q_i^j$ and $Q_i^k$ are identifiable when only $N$ nodes are considered. That is, from Definition 1, $\overline{S_i^j(N)} \cap \overline{S_i^k(N)} = \emptyset$, where $N$ indicates the number of nodes involved in the merging process. Note that since every element $\mathbf{Q}^j(M) = (Q_1, ..., Q_N, Q_{N+1}, ..., Q_M) \in S_i^j(M)$ is constructed by concatenating $M - N$ indices $Q_{N+1}, ..., Q_M$ with the corresponding element, $\mathbf{Q}^j(N) = (Q_1, ..., Q_N) \in S_i^j(N)$, we have that $\mathbf{Q}^j(M) \neq \mathbf{Q}^k(M)$ if $\mathbf{Q}^j(N) \neq \mathbf{Q}^k(N)$. Thus, by the property of the intersection operator $\cap$, we can claim that $\overline{S_i^j(M)} \cap \overline{S_i^k(M)} = \emptyset \quad \forall M \geq N$, implying that $Q_i^j$ and $Q_i^k$ are still identifiable even when we consider M nodes.

Thus, we can start the merging process with just two nodes and continue to do further merging by adding one node (or a few) at a time without change in previously merged bins. When many nodes are involved, this would lead to significant savings in computational complexity. In addition, if some of the nodes are located far away from the nodes being added (that is, the dynamic ranges of their quantizers do not overlap with those of the nodes being added), they can be skipped for further merging without loss of merging performance.

## 4.6 Extension of Identifiability: p-identifiability

Since for real operating conditions, there exist measurement noise ($w_i \neq 0$) and/or parameter mismatches, the assumption that $Pr[(Q_1, ..., Q_M) \in S_Q] = 1$ is no longer valid. Thus, we need to consider modifications to the merging technique to allow it to operate under noisy condition. We start by constructing the set $S_Q$ by taking elements in $S_M$ that have high probabilities. In other words, we discard some $M$-tuples in $S_M$ that rarely happen so that we can maintain $Pr[\mathbf{Q}_r \in S_Q(p)] = p(\simeq 1)$ and still achieve good rate savings by the merging technique. Formally,

$$S_Q(p) = \{\mathbf{Q}_{(1)}, ..., \mathbf{Q}_{(|S_Q(p)|)}\}, \quad Pr[\mathbf{Q}_{(i)}] \geq Pr[\mathbf{Q}_{(j)}] \quad i < j, \quad i, j = 1, ..., |S_M| \qquad (4.7)$$

Notice that a decoding error will occur at the fusion node whenever an element in $S_M - S_Q(p)$ is produced. Clearly, there will be trade-off between rate savings and decoding errors. If we choose $S_Q(p)$ to be as small as possible, we can achieve better rate savings at the expense of larger decoding error, which could lead to significant degradation of localization performance. Handling of decoding errors will be discussed in Section 4.7.

With this consideration, Definition 1 can be restated as follows:

**Definition 2** *$Q_i^j$ and $Q_i^k$ are p-identifiable, and therefore can be merged, iff $\overline{S_i^j}(p) \cap \overline{S_i^k}(p) = \emptyset$,*

where $\overline{S_i^j}(p)$ and $\overline{S_i^k}(p)$ are constructed from $S_Q(p)$. Notice that $p$-identifiability allows us to apply the merging technique explained in Section 4.5 and thus achieve good rate

savings at the expense of decoding error. Clearly, the probability of decoding error would be less than $1 - p$.

## 4.7 Decoding of Merged Bins and Handling Decoding Errors

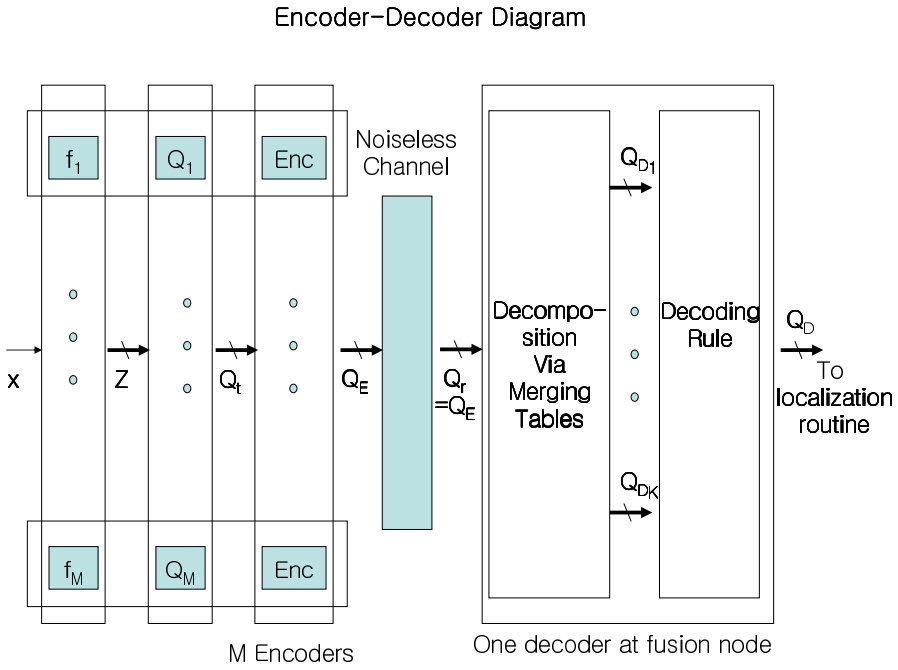


Figure 4.1: Encoder-Decoder Diagram

When there is a decoding error, the first step we should take would be to obtain the possible M-tuples, $\mathbf{Q}_{D_1}, ..., \mathbf{Q}_{D_K}$ from the received M-tuple $\mathbf{Q}_r$ (encoded version) by using the $M$ merging tables. Note that the merging process is done off-line in a centralized manner. In real operation, each node stores its merging table to perform the encoding and the fusion node uses $S_Q(p)$ and $M$ merging tables to do the decoding. For example when $M = 3, R_i = 2$, suppose that according to node 1's merging table, $Q_1^1$ and $Q_1^4$ can be merged into $Q_1^1$, implying that node 1 will transmit $Q_1^1$ to the fusion node whenever

$z_1$ belongs to $Q_1^1$ or $Q_1^4$. If the fusion node receives $\mathbf{Q}_r = (1, 2, 4)$, it decomposes $(1, 2, 4)$ into $(1, 2, 4)$ and $(4, 2, 4)$ by using node 1's merging table. This decomposition will be performed for the other $M - 1$ merging tables.

Suppose we have a set of K M-tuples, $S_D = \{\mathbf{Q}_{D_1}, ..., \mathbf{Q}_{D_K}\}$ decomposed from $\mathbf{Q}_r$. Then clearly, $\mathbf{Q}_r \in S_D$ and $\mathbf{Q}_t \in S_D$ where $\mathbf{Q}_t$ is the true M-tuple before encoding (see Figure 4.1). It is observed that since the decomposed M-tuples are produced via the M merging tables from the true one, $\mathbf{Q}_t$, it is very likely that $\Pr(\mathbf{Q}_{D_k}) \ll 1$, where $\mathbf{Q}_{D_k} \neq \mathbf{Q}_t, \quad k = 1, ..., K$. In other words, since the encoding process allows us to merge the quantization bins whenever any M-tuples that contain either of them are very unlikely to happen at the same time, the M-tuples, $\mathbf{Q}_{D_k} (\neq \mathbf{Q}_t)$, tend to take very low probability.

### 4.7.1 Decoding Rule 1: Simple Maximum Rule

Since the received M-tuple $\mathbf{Q}_r$ has ambiguity produced by encoders at each node, the decoder at fusion node should be able to find the true M-tuple by using appropriate decoding rules. As a simple rule, we can take the M-tuple (out of $\mathbf{Q}_{D_1}, ..., \mathbf{Q}_{D_K}$) that is most likely to happen. Formally,

$$\mathbf{Q}_D = \arg\max_k Pr[\mathbf{Q}_{D_k}], \quad k = 1, ..., K \tag{4.8}$$

where $\mathbf{Q}_D$ is the decoded M-tuple which will be forwarded to the localization routine. Now we consider two possible cases as follows:

- $\mathbf{Q}_t \in S_Q(p)$

  There will be no decoding error and there exists only one $M$-tuple $\mathbf{Q}_D$ from K

$M$-tuples that belongs to $S_Q(p)$. Note that $Pr[\mathbf{Q}_D] \geq Pr[\mathbf{Q}_{D_k}] \quad k = 1, ..., K$ due to the property of $S_Q(p)$ in (4.7) and thus the decoding rule in (4.8) allows us to obtain $\mathbf{Q}_t$ out of K $M$-tuples without decoding error.

- $\mathbf{Q}_t \in S_M - S_Q(p)$

  Since the decoding error occurs only when $Pr[\mathbf{Q}_t] < Pr[\mathbf{Q}_D]$, the decoding error probability will be less than $1 - p$. Note that $Pr[\mathbf{Q} \in S_Q(p)] = p$.

### 4.7.2 Decoding Rule 2: Weighted Decoding Rule

Instead of choosing only one decoded M-tuple, we can treat each decomposed M-tuple as a candidate for decoding with a corresponding weight based on likelihood. For example, we can view $\mathbf{Q}_{D_k}$ as the decoded M-tuple with weight of $W_k = \frac{Pr[\mathbf{Q}_{D_k}]}{\sum_l^K Pr[\mathbf{Q}_{D_l}]} \quad k = 1, ..., K$. It should be noted that the weighted decoding rule will be used along with the localization routine as follows:

$$\hat{\mathbf{x}} = \sum_k^K \hat{\mathbf{x}}_k W_k \quad k = 1, ..., K \tag{4.9}$$

where $\hat{\mathbf{x}}_k$ is the estimated source location using the decoded M-tuple, $\mathbf{Q}_{D_k}$. For simplicity, we can take a few dominant M-tuples for the weighted decoding and localization. That is,

$$\hat{\mathbf{x}} = \sum_k^L \hat{\mathbf{x}}_{(k)} W_{(k)} \quad k = 1, ..., L \tag{4.10}$$

where $W_{(k)}$ is the weight of $\mathbf{Q}_{D_{(k)}}$ and $Pr[\mathbf{Q}_{D_{(i)}}] \geq Pr[\mathbf{Q}_{D_{(j)}}]$ if $i < j$. Typically $L$ is chosen as a small number (e.g., $L = 2$). Note that the weighted decoding rule with $L = 1$ is equivalent to the simple maximum rule in (4.8).

## 4.8 Application to Acoustic Amplitude Sensor Case

In order to perform distributed encoding at each node, we first need to obtain the set $S_Q$, which can be constructed from (4.1) as follows:

$$S_Q = \{(Q_1, ..., Q_M) | \ \exists \mathbf{x} \in S, Q_i = \alpha_i(g_i \frac{a}{\| \mathbf{x} - \mathbf{x}_i \|^\alpha} + w_i)\} \tag{4.11}$$

where the $i$-th sensor reading $z_i(\mathbf{x})$ is expressed by the sensor model $g_i \frac{a}{\|\mathbf{x}-\mathbf{x}_i\|^\alpha}$, and the measurement noise, $w_i$ (see Section 2.5.1 for further details about the expression). When the signal energy $a$, is known and there is no measurement noise ($w_i = 0$), it would be straightforward to construct the set $S_Q$. That is, each element in $S_Q$ corresponds to one region in sensor field which is obtained by computing the intersection, $A$, of M ring-shaped areas, $A_1, ..., A_M$. For example, using an j-th element $\mathbf{Q}^j = (Q_1^j, ..., Q_M^j)$ in $S_Q$, we can compute the corresponding intersection $A^j$ as follows:

$$A_i = \{\mathbf{x} | g_i \frac{a}{\| \mathbf{x} - \mathbf{x}_i \|^\alpha} \in Q_i^j, \mathbf{x} \in S\}, \quad i = 1, ..., M \tag{4.12}$$

$$A^j = \bigcap_i^M A_i \tag{4.13}$$

Clearly, since the nodes involved in localization of any given source location generate the same M-tuple, the set $S_Q$ will be computed deterministically. In other words, $Pr[\mathbf{Q} \in S_Q] = 1$. Thus, using $S_Q$, we can apply our merging technique to this case and achieve significant rate savings without any degradation of localization accuracy (no decoding error).

However, measurement noise and/or unknown signal energy will make this problem complicated by allowing random realizations of M-tuples generated by M nodes for any given source location. Since the condition for no decoding error, i.e., $Pr[\mathbf{Q} \in S_Q] = 1$, is satisfied only when $S_Q$ takes all possible M-tuples, the size of $S_Q$ should be increased to reduce the decoding errors and this will result in large reduction in the rate savings achieved by our encoding algorithm. Thus, by noting that the decoding errors will occur whenever $\mathbf{Q}_r \in S_M - S_Q$, we can construct $S_Q$ by including only those elements with high probability, so that decoding errors are unlikely. Formally, we construct $S_Q(p)$ such that $Pr[\mathbf{Q} \in S_Q(p)] = p(\approx 1)$ and then apply our modified merging algorithm with p-identifiability explained in Section 4.6.

### 4.8.1 Construction of $S_Q(p)$

In order to construct $S_Q(p)$, which should meet the property (4.7), we need to have all possible M-tuples and compute their probabilities to obtain the sorted version of $\mathbf{Q}_{(1)}, ..., \mathbf{Q}_{(|S_Q|)}$. Practically, since this would incur very large computation cost, we instead construct $S_Q$ as follows:

- Assuming no measurement noise, construct multiple $S_Q(a_k)$'s using (4.11) where $a = a_k, w_i = 0, k = 1, ..., L_a$. Note that $L_a = \frac{a_{max} - a_{min}}{\Delta a}$, and $\Delta a = a_{k+1} - a_k$ is chosen as a small value ($\ll 1$).

- Check if $Pr[\mathbf{Q} \in S_Q(p) = \bigcup_{k=1}^{L_a} S_Q(a_k)] = p$.

- Otherwise, generate random realizations of M-tuples by using measurement noise until $Pr[\mathbf{Q} \in S_Q(p)] = p$.

Note that this construction allows $S_Q(p)$ to take most of M-tuples with high probability due to the assumption of normal distribution of measurement noise.

## 4.9 Experimental results

The distributed encoding algorithm is applied to the system where each node employs an acoustic amplitude sensor model for source localization. The experimental results are provided in terms of average localization error, $E\|\mathbf{x}-\hat{\mathbf{x}}\|^2$, and rate savings (%) computed by $\frac{R_T-R_M}{R_T} \times 100$, where $R_T$ is the rate consumed by M nodes when only the independent entropy coding (Huffman coding) is applied after quantization and $R_M$ is the total rate computed when the merging technique is applied before entropy coding. In performing the localization based on the quantized noisy sensor readings, the localization algorithm proposed in Chapter 3 was applied to compute $E\|\mathbf{x}-\hat{\mathbf{x}}\|^2$.

We also assume that each node uses the quantizer (LSQ) proposed in Chapter 2 except for the experiments where otherwise noted.

### 4.9.1 Distributed Encoding Algorithm

First, we assume that each node can measure the known signal energy without measurement noise. The distributed encoding algorithm proposed in Section 4.5 has been applied to the acoustic sensor system. Figure 4.2 shows the overall performance of the system for each quantization scheme. In this experiment, 100 different 5-node configurations were generated in a sensor field $10 \times 10m^2$. For each configuration, a test set of 2000 random source locations was used to obtain sensor readings, which are then quantized by three different quantizers, namely, uniform quantizers, Lloyd quantizers and LSQs. The

average localization error and total rate $R_M$ are averaged over 100 node configurations. As expected, the overall performance for LSQ is the best of all since the total reduction in redundancy can be maximized when the application-specific quantization (LSQ) and the distributed encoding are used together.

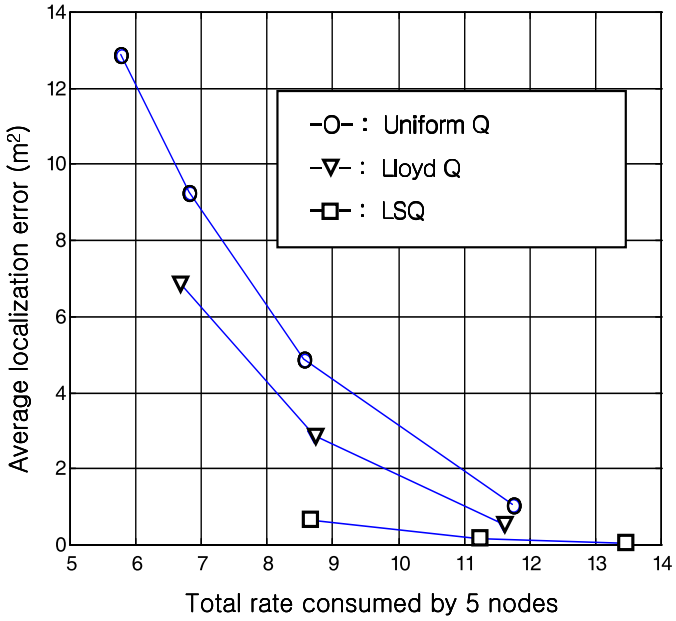


Figure 4.2: Average localization error vs. Total rate $R_M$ for three different quantization schemes with distributed encoding algorithm. Average rate savings is achieved by the distributed encoding algorithm (global merging algorithm).

Our encoding algorithm with the different merging techniques outlined in Section 4.5 is applied for comparison and the results are provided in Table 4.1. Methods 1 and 2 are as described in Section 4.5, and Method 3 is the global merging algorithm discussed in that section. We can observe that even with relative low rates (4 bits per node) and a small number of nodes (only 5) significant rate gains (up to 30%) can be achieved with our merging technique.

Table 4.1: Total rate, $R_M$ in bits (Rate savings) achieved by various merging techniques.

| $R_i$ | Method 1 | Method 2 | Method 3 |
|---|---|---|---|
| 2 | 9.4 (8.7%) | 9.4 (8.7%) | 9.10 (11.6%) |
| 3 | 11.9 (20.6%) | 12.1 (19.3%) | 11.3 (24.6%) |
| 4 | 13.7 (31.1%) | 14.1 (29.1%) | 13.6 (31.6%) |

The encoding algorithm was also applied to many different node configurations to characterize the performance. In this experiment, 500 different node configurations were generated for each $M(M = 3, 4, 5)$ in a sensor field $10 \times 10m^2$. After quantization, the global merging technique has been applied to obtain the rate savings. In obtaining the metric in (4.6), the source distribution is assumed to be uniform. The average rate savings achieved by the encoding algorithm is computed as a sample mean over 500 different node configurations and plotted in Figure 4.3. Note that the performance of our encoding algorithm is dependent upon the set $S_Q$ given by (4.1).

Since there are a large number of nodes in a typical sensor network, our distributed algorithms have been applied to the system with an acoustic sensor model in a larger sensor field ($20 \times 20m^2$). In this experiment, 20 different node configurations are generated for each $M(= 12, 16, 20)$ and for each node configuration, our encoding algorithm is applied after quantization with assumption of no measurement noise. Note that the node density for $M = 20$ in $20 \times 20m^2$ is equal to $\frac{20}{20 \times 20} = 0.05$ which is also the node density for the case of $M = 5$ in $10 \times 10m^2$. In Table 4.2 it is worth noting that the system with a larger number of nodes outperforms the system with a smaller number of nodes ($M = 3, 4, 5$) although the node density is kept the same. This is because the incremental property of the merging technique allows us to find more identifiable bins at each node.

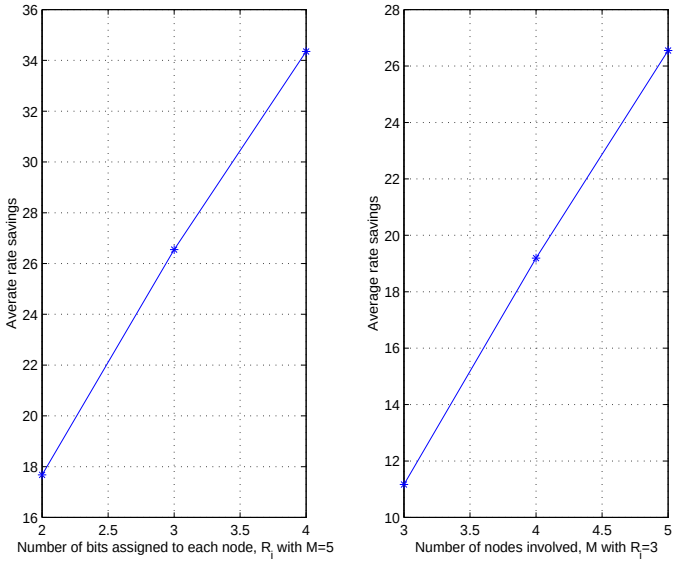


Figure 4.3: Average rate savings achieved by the distributed encoding algorithm (global merging algorithm) vs. number of bits, $R_i$ with $M = 5$ (left) and number of nodes with $R_i = 3$ (right)

Table 4.2: Total rate $R_M$ in bits (Rate savings) achieved by distributed encoding algorithm (global merging technique). The rate savings is averaged over 20 different node configurations where each node uses LSQ with $R_i = 3$.

| $M$ | Total rate $R_M$ in bits (Rate savings) |
|---|---|
| 12 | 17.3237 (51.56%) |
| 16 | 20.7632 (56.45%) |
| 20 | 23.4296 (60.69%) |

### 4.9.2 Encoding with p-Identifiability and Decoding rules

The distributed encoding algorithm with p-identifiability described in Section 4.6 was applied to the case where each node collects noise-corrupted measurements of unknown source signal energy. First, assuming known signal energy, we checked the effect of measurement noise on the rate savings, and thus decoding error by varying the size of $S_Q(p)$ (see Figure 4.4). In this experiment, the variance of measurement noise, $\sigma^2$, varies from

0 to $0.5^2$ and for each $\sigma^2$, a test set of 2000 source locations was generated with $a = 50$. Figure 4.4 illustrates that good rate savings can be still achieved in a noisy situation at the expense of a small decoding error. Clearly, it can be noted that better rate savings can be achieved at higher SNR[3] and (or) with a larger decoding error ($< 0.05$) allowed.

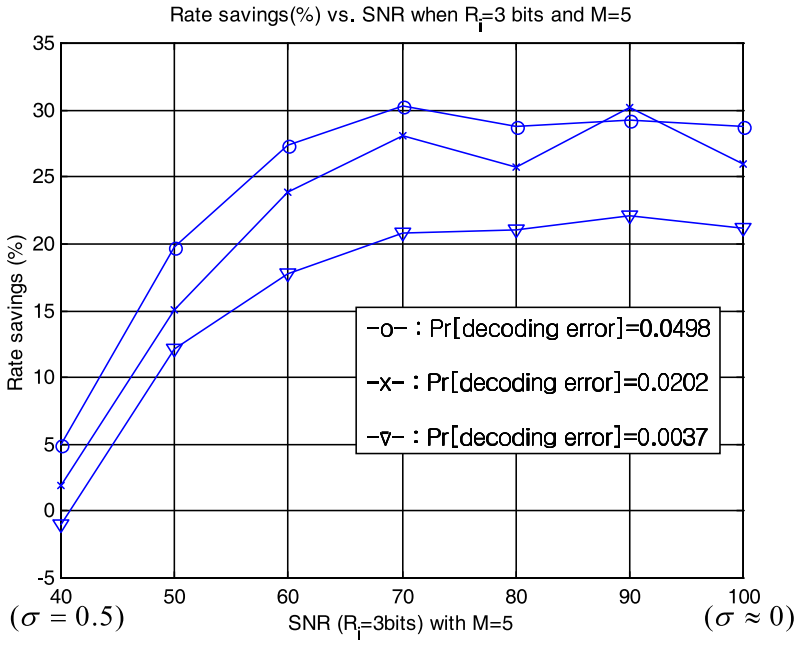


Figure 4.4: Rate savings achieved by the distributed encoding algorithm (global merging algorithm) vs. SNR (dB) with $R_i = 3$ and M=5. $\sigma^2 = 0, ..., 0.5^2$

For the case of unknown signal energy where we assume that $a \in [a_{min} \quad a_{max}]$, we constructed $S_Q(p) = \bigcup_{k=1}^{L_a} S_Q(a_k)$ with $\Delta a = a_{k+1} - a_k = \frac{a_{max} - a_{min}}{L_a} = 0.5$ by varying $p = 0.8, ..., 0.95$ where $S_Q(a_k)$ is the set $S_Q$ constructed when $a = a_k$ in noise-free condition ($w_i = 0$). Using $S_Q(p)$, we applied the merging technique with p-identifiability to evaluate the performance (rate savings vs. localization error). In the experiment, a test set of 2000 samples is generated from uniform priors for $p(\mathbf{x})$ and $p(a)$ with each

[3]Note that for practical vehicle target, the SNR is often much higher than 40dB [19].

noise variance ($\sigma = 0, 0.05$). In order to deal with decoding errors, two decoding rules in Section 4.7 were applied along with the localization algorithm in Chapter 3. In Figure 4.5, the performance curves for two decoding rules were plotted for comparison. As can be seen, the weighted decoding rule performs better than the simple maximum rule since the former takes into account the effect of the other decomposed M-tuples on localization accuracy by adjusting their weights. It is also noted that when decoding error is very low (equivalently, $p \approx 1$), both of them show almost the same performance.

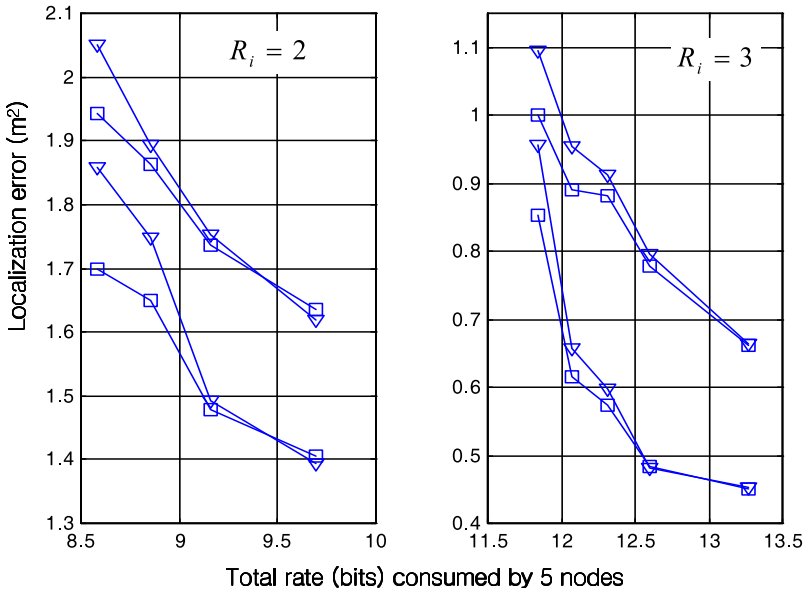


Figure 4.5: Average localization error vs. total rate $R_M$ achieved by the distributed encoding algorithm (global merging algorithm) with simple maximum decoding and weighted decoding, respectively. Total rate varies by changing $p$ from 0.8 o 0.95 and weighted decoding is conducted with $L = 2$. Solid line + $\square$: weighted decoding. Solid line + $\nabla$: simple maximum decoding.

To see how much gain we can obtain from the encoding, we compared this to the system which uses only the entropy coding without applying the merging technique.

In Figure 4.6, the performance curves are plotted by changing the size of $S_Q(p)$ with $\sigma = 0, 0.05$. It should be noted that we can determine the size of $S_Q(p)$ (equivalently, $p$) that provides the best performance from this experiment.

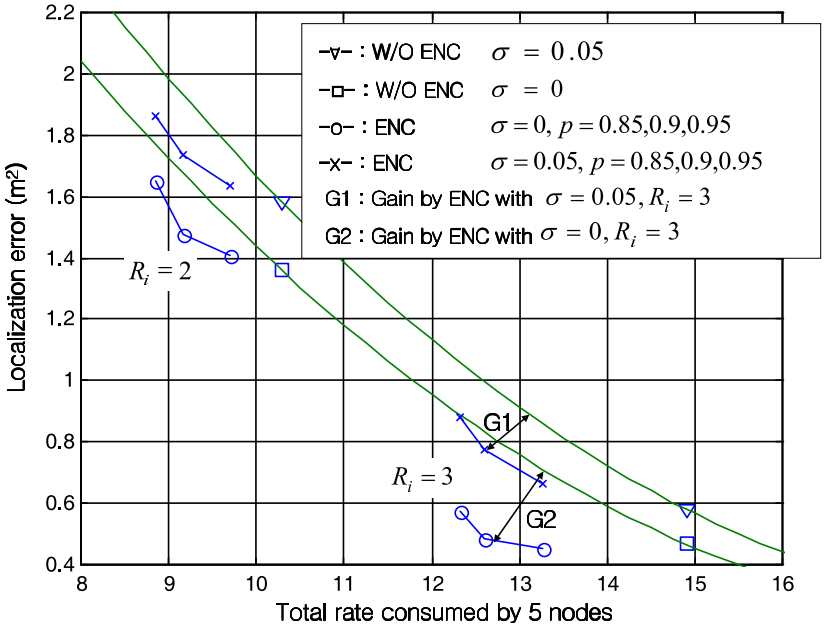


Figure 4.6: Average localization error vs. total rate, $R_M$ achieved by the distributed encoding algorithm (global merging algorithm) with $R_i = 3$ and M=5. $\sigma = 0, 0.05$. $S_Q(p)$ is varied from $p = 0.85, 0.9, 0.95$. Weighted decoding with $L = 2$ is applied in this experiment.

### 4.9.3 Performance Comparison: Lower Bound

We address the question of how our technique compares with the best achievable performance for this source localization scenario. As a bound on achievable performance we consider a system where (i) each node quantizes its observation independently and (ii) the quantization indices generated by all nodes for a given source location are jointly coded (in our case we use the joint entropy of the vector of observations as the rate estimate).

This approach can be applied to both the original quantizer designed and the quantizer obtained after merging.

Note that this is not a realistic bound because joint coding cannot be achieved unless the nodes are able to communicate before encoding. Note that in order to approximate the behavior of the joint entropy coder via distributed source coding techniques one would have to transmit multiple observations of the source energy from each node, as the source is moving around the sensor field. Some of the nodes could send observations that are directly encoded, while others could transmit a syndrome produced by an error correcting code based on the quantized observations. Then, as the fusion node receives all the information from the various nodes it would be able to exploit the correlation from the observations and approximate the joint entropy. This method would not be desirable, however, because the information in each node depends on the location of the source and thus to obtain a reliable estimate of the measurement at all nodes one would have to have observations at a sufficient number of positions of the source. Thus, instantaneous localization of the source would not be possible. The key point here, then, is that the randomness between observations across nodes is based on the localization of the source, which is precisely what we wish to observe.

For one 5-node configuration, the average rate per node was plotted with respect to the localization error in Figure 4.7, with assumption of no measurement noise ($w_i = 0$) and known signal energy. As can be seen from Figure 4.7, our distributed encoding algorithm in Section 4.5 outperform techniques based on uniform quantization. For this particular configuration we can observe a gap of less than 1 bit/node, at high rates, between the performance achieved by proposed quantizer with distributed encoding and

that achievable with the same quantizer if joint entropy coding was possible. In summary, our merging technique with the proposed quantization scheme provides substantial gain over straightforward application of known techniques and comes close to the optimal achievable performance.

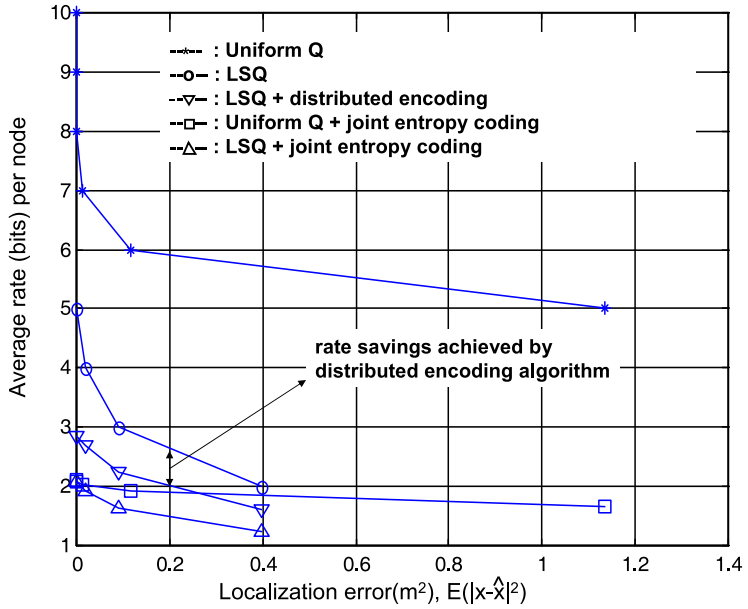


Figure 4.7: Performance comparison: distributed encoding algorithm is lower bounded by joint entropy coding.

## 4.10 Conclusion

Using the distributed property of the quantized observations, we proposed a novel encoding algorithm which allows us to obtain significant rate savings by merging quantization bins. We also developed decoding rules to deal with the decoding errors which can be caused by measurement noise and/or parameter mismatches. In the experiment, we showed that the system equipped with the quantizers proposed in Chapter 2 and the

distributed encoders achieved significant data compression as compared with standard systems.

# Chapter 5

# Conclusion and Future work

In this thesis, we have studied the impact of quantization on the performance of source localization systems where distributed sensors measure source signals, quantize the noise-corrupted measurements, encode them and send them to a fusion node that performs decoding and the localization based on quantized data to estimate the source location.

We proposed an iterative design algorithm which allows us to reduce the localization error for quantizer design. We showed that quantizer design should be "application-specific". We addressed the rate allocation problem and showed that the rate allocation result could be improved by taking into account the quantization scheme at each sensor. We also proposed a novel distributed encoding algorithm that merges quantization bins at each sensor whenever the ambiguity created by this merging can be resolved at the fusion node by using information from other sensors.

As an example of the localization application, we considered an acoustic amplitude sensor system where each sensor measures the source signal energy based on an energy decay sensor model. For this application, we proposed a distributed localization algorithm based on the maximum a posteriori (MAP) criterion. We showed that the localization

algorithm achieves good performance with reasonable complexity as compared to the minimum mean squared error (MMSE) estimation.

Extensive simulations have been conducted to characterize the performance of our distributed algorithms. They demonstrated the benefits of using application-specific designs to replace traditional quantizers such as uniform quantizers and Lloyd quantizers. They also showed that the rate allocation optimized for source localization achieved significant gains as compared to a uniform rate allocation. In addition, the experiments showed the complexity of the localization algorithm could be significantly reduced by taking into account the distributed property of the quantized data without much degradation of the localization accuracy. They also showed that significant rate savings could be achieved via our encoding algorithm.

In future work, many relevant topics and ideas can be addressed. First, in this thesis, we have considered a specific source localization system and used the simulation based data to test our algorithms. Thus, it would be worth applying the algorithms to real data obtained in the test ground for various systems where different types of sensors can be employed at each sensor for different tasks. Second, we assumed that the communication link between the sensors and the fusion node is fully reliable. Further work should be conducted to incorporate the noisy link to our design framework. Third, the topic that can be addressed is the joint design of quantizers and encoders since there exists dependency between quantization and encoding of quantized data which will be exploited to obtain more performance gain. Finally, complexity should be addressed for practical applications. Note that our design algorithms operate off-line by using information of sensor locations. However, in many cases of interest the sensor network could

be reconfigured regularly and would require on-line tasks. In these cases, low complexity techniques would be very important.

# Bibliography


[1] D. Blatt and A. O. Hero. Energy based sensor network source localization via projection onto convex sets (POCS). *IEEE Transactions on Signal Processing*, 54(9):3614–3619, September 2006.

[2] J. C. Chen, R. E. Hudson, and K. Yao. Maximum-likelihood source localization and unknown sensor location estimation for wideband signals in the near-field. *IEEE Transactions on Signal Processing*, 50(8):1843–1854, August 2002.

[3] J. C. Chen, K. Yao, and R. E. Hudson. Source localization and beamforming. *IEEE Signal Processing Magazine*, 19(2), March 2002.

[4] J. C. Chen, K. Yao, and R. E. Hudson. Acoustic source localization and beamforming: Theory and practice. *EURASIP Journal on Applied Signal Processing*, pages 359–370, 2003.

[5] J. C. Chen, L. Yip, J. Elson, H. Wang, D. Maniezzo, K. Yao, R. E. Hudson, and D. Estrin. Coherent acoustic array processing and localization on wireless sensor networks. In *IEEE Proceedings*, August 2003.

[6] P. A. Chou, T. Lookabaugh, and R. M. Gray. Entropy-constrained vector quantization. *IEEE Trans. on Acoustic, Speech, and Signal processing*, pages 31–41, January 1989.

[7] T. M. Cover and J.A.Thomas. *Elements of Information Theory*. Wiley-Interscience Publication, 1991.

[8] T. J. Flynn and R. M. Gray. Encoding of correlated observations. *IEEE Trans. on Information Theory*, November 1987.

[9] P. Frossard, O. Verscheure, and C. Venkatramani. Signal processing challenges in distributed stream processing systems. In *IEEE International Conference on Acoustic, Speech, and Signal Processing (ICASSP)*, Toulouse, France, May 2006.

[10] P. H. Garthwaite, I. T. Jolliffe, and B. Jones. *Statistical Inference - Second Edition*. Oxford University Press, 2002.

[11] A. O. Hero and D. Blatt. Sensor network source localization via projection onto convex sets (POCS). In *IEEE International Conference on Acoustic, Speech, and Signal Processing (ICASSP)*, March 2005.

[12] P. Ishwar, R. Puri, K. Ramchandran, and S. S. Pradhan. On rate-constrained distributed estimation in unreliable sensor networks. *IEEE Journal on Selected Areas in Communications*, 23:765– 775, April 2005.

[13] V. Isler and R. Bajcsy. The sensor selection problem for bounded uncertainty sensing models. In *IEEE International symposium on Information Processing in Sensor Networks (IPSN)*, April 2005.

[14] S. M. Kay. *Fundamentals of Statistical Signal Processing*. Prentice-Hall Inc., New Jersey, 1993.

[15] Y. H. Kim. and A. Ortega. Quantizer design and distributed encoding algorithm for source localization in sensor networks. In *IEEE International symposium on Information Processing in Sensor Networks (IPSN)*, April 2005.

[16] Y. H. Kim. and A. Ortega. Quantizer design for source localization in sensor networks. In *IEEE International Conference on Acoustic, Speech, and Signal Processing (ICASSP)*, March 2005.

[17] Y. H. Kim. and A. Ortega. Maximun a posteriori (MAP)-based algorithm for distributed source localization using quantized acoustic sensor readings. In *IEEE International Conference on Acoustic, Speech, and Signal Processing (ICASSP)*, May 2006.

[18] Y. H. Kim and A. Ortega. Quantizer design and rate allocation for source localization in sensor networks. *Submitted to IEEE Transactions on Signal Processing*, 2007.

[19] D. Li and Y. H. Hu. Energy-based collaborative source localization using acoustic microsensor array. *EURASIP Journal on Applied Signal Processing*, pages 321–337, 2003.

[20] D. Li, K. D. Wong, Y. H. Hu, and A. M. Sayeed. Detection, classification and tracking of targets. *IEEE Signal Processing Magazine*, 19(2):17–29, March 2002.

[21] M. Lightstone and S. K. Mitra. Optimal variable-rate mean-gain-shape vetor quantization for image coding. *IEEE Trans. on Circuits and Systems for Video Technology*, pages 660–668, December 1996.

[22] J. Liu, J. Reich, and F. Zhao. Collaborative in-network processing for target tracking. *EURASIP Journal on Applied Signal Processing*, pages 378–391, 2003.

[23] Z.-Q. Luo. Universal decentralized estimation in a bandwidth constrained sensor network. *IEEE Trans. on Information Theory*, pages 2210–2219, June 2005.

[24] C. Meesookho, U. Mitra, and S. Narayanan. Distributed range difference based target localization in sensor networks. In *Proceedings of Asilomar Conference on Signals, Systems and Computers*, Pacific Grove, CA, October 2005.

[25] R. Niu and P. K. Varshney. Target location estimation in wireless sensor networks using binary data. In *Proceedings of the 38th Annual Conference on Information Sciences and Systems*, Princeton, NJ, March 2004.

[26] R. Niu and P. K. Varshney. Target location estimation in sensor networks with quantized data. *IEEE Transactions on Signal Processing*, 54(12):4519–4528, December 2006.

[27] T. S. Rappaport. *Wireless Communications:Principles and Practice*. Prentice-Hall Inc., New Jersey, 1996.

[28] E. A. Riskin. Optimal bit allocation via the generalized BFOS algorithm. *IEEE Trans. on Information Theory*, 37:400–402, March 1991.

[29] K. Sayood. *Introduction to Data Compression - Second Edition*. Morgan Kaufmann Publishers, 2000.

[30] X. Sheng and Y. H. Hu. Maximum-likelihood multiple-source localization using acoustic energy measurements with wireless sensor networks. *IEEE Transactions on Signal Processing*, 53(1):44–53, January 2005.

[31] J. O. Smith and J. S. Abel. Closed-form least-squares source location estimation from range-difference measurements. *IEEE Trans. on Acoustics, Speech and Signal Processing*, pages 1661–1669, December 1987.

[32] N. Srinivasamurthy and A. Ortega. Joint compression-classification with quantizer/classifier dimension mismatch. In *Visual Communications and Image Processing 2001*, San Jose, CA, Jan. 2001.

[33] N. Srinivasamurthy, A. Ortega, and S. Narayanan. Towards optimal encoding for classification with applications to distributed speech recognition. In *Proc. of Eurospeech*, http://sipi.usc.edu/∼ortega/Papers/NaveenEuro03.pdf, Geneva, September 2003.

[34] N. Srinivasamurthy, A. Ortega, and S. Narayanan. Efficient scalable encoding for distributed speech recognition. *Speech Communication*, 48:888–902, 2006.

[35] I. H. Tseng, O. Verscheure, D. S. Turaga, and U. V. Chaudhari. Quantization for adapted GMM-based speaker verification. In *IEEE International Conference on Acoustic, Speech, and Signal Processing (ICASSP)*, Toulouse, France, May 2006.

[36] L. Vasudevan, A. Ortega, and U. Mitra. Application-specific compression for time delay estimation in sensor networks. In *First ACM Conference on Embedded Networked Sensors*, Los Angeles, CA, Nov 2003.

[37] L. Vasudevan, A. Ortega, and U. Mitra. Jointly optimized quantization and time delay estimation for sensor networks. In *First Intl. Symposium on Control, Communications, and Signal Processing*, Tunisia, March 2004.

[38] H. Wang, K. Yao, G. Pottie, and D. Estrin. Entropy-based sensor selection heuristic for target localization. In *IEEE International symposium on Information Processing in Sensor Networks (IPSN)*, 2004.

[39] J.-J. Xiao, S. Cui, Z.-Q. Luo, and A. Goldsmith. Joint estimation in sensor networks under energy constraints. In *IEEE First Conference on Sensor and Ad Hoc Communications and Networks*, October 2004.

[40] J.-J. Xiao, A. Ribeiro, Z.-Q. Luo, and G. B. Giannakis. Distributed compression-estimation using wireless sensor networks. *IEEE Signal Processing Magazine*, 23(4):27–41, July 2006.

[41] H. Yang and B. Sikdar. A protocol for tracking mobile targets using sensor networks. In *Proceedings of IEEE Workshop on Sensor Network Protocols and Applications*, Anchorage, AK, May 2003.

[42] F. Zhao, J. Shin, and J. Reich. Information-driven dynamic sensor collaboration for target tracking. *IEEE Signal Processing Magazine*, 19(2):61–72, March 2002.